Measurements of Stratified Turbulence in Mountain Terrain. Bursting pnenomena.

Eliezer Kit
School of Mechanical Engineering,
Tel-Aviv University

In collaboration with: Joe Fernando
Chris Hocut
Dan Liberzon

Motivation and Layout of the talk

- Fine resolution measurements of atmospheric turbulence, which enable to determine dissipation, velocity derivatives etc. using a combo instrument (multi-sensor hot films embedded within a sonic).
- The use of in-situ calibration by utilizing a low resolution data from Sonic and NN procedure.
- Experimental results on stratified turbulence from fall campaign. Transition from stratified turbulence to Kolmogorov turbulence.
- Bursting phenomena. Internal waves and their breaking as path to bursting. Just thoughts.
- Conclusions

- **DUGWAY FALL RESULTS**
- **STRATIFIED TURBULENCE**
- **BURSTING**

Combo Probe Placement

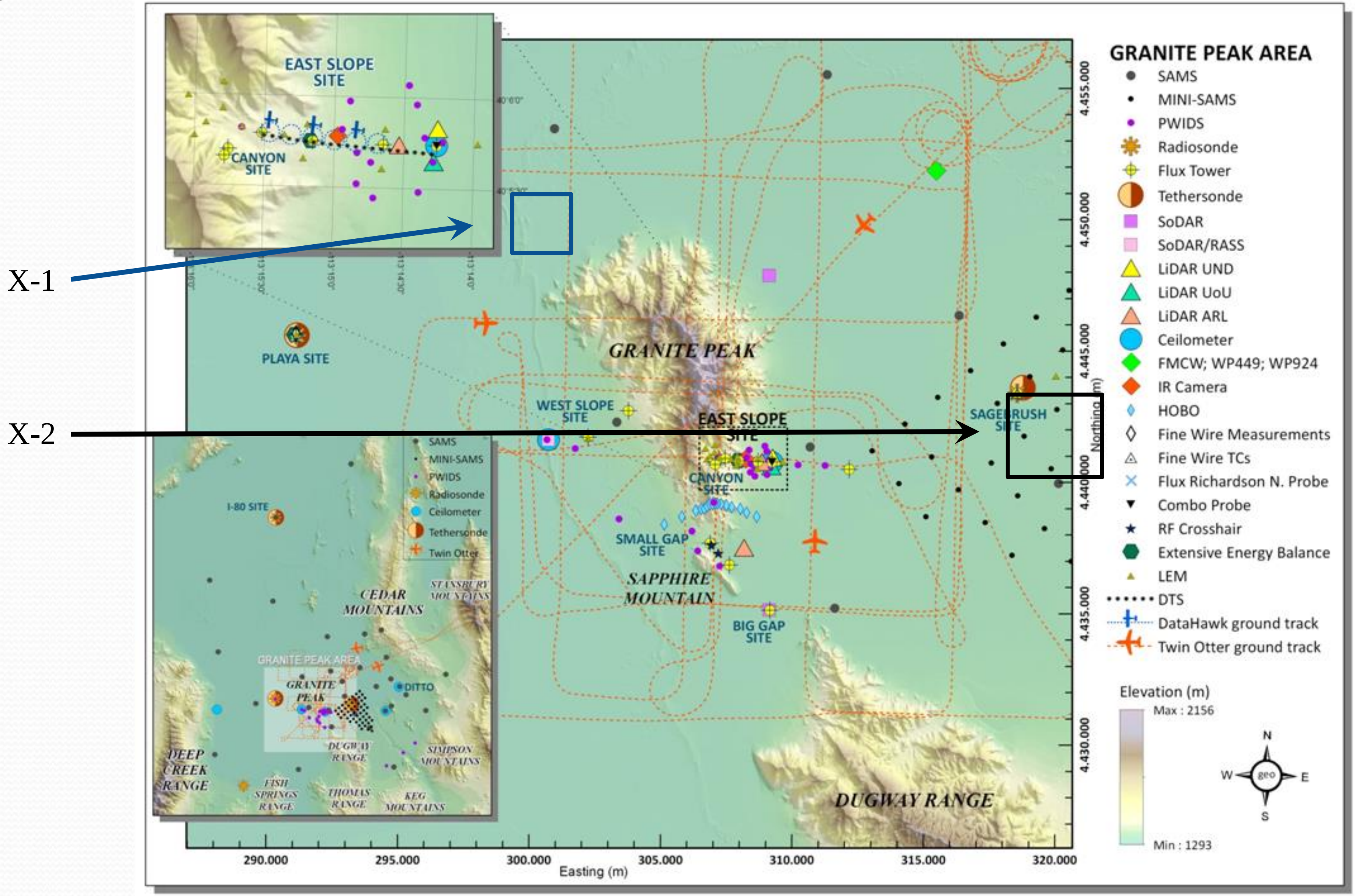

MATERHORN-X: ES2 tower. Combos at 2 and 6 m

Combo probes located at 2m and 6m

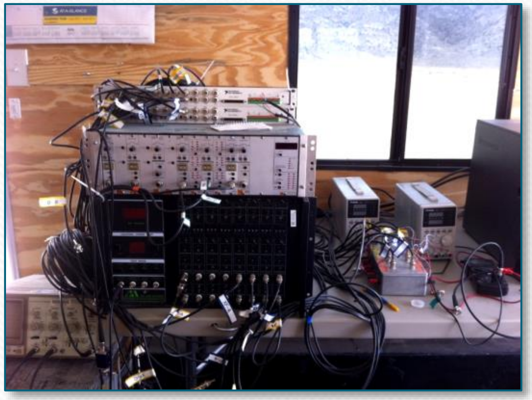

Combo probe electronics

Wind speed at the ES-2 tower (10/19/2012). At 22:00 MDT, wind speed rapidly increased as the flow developed.

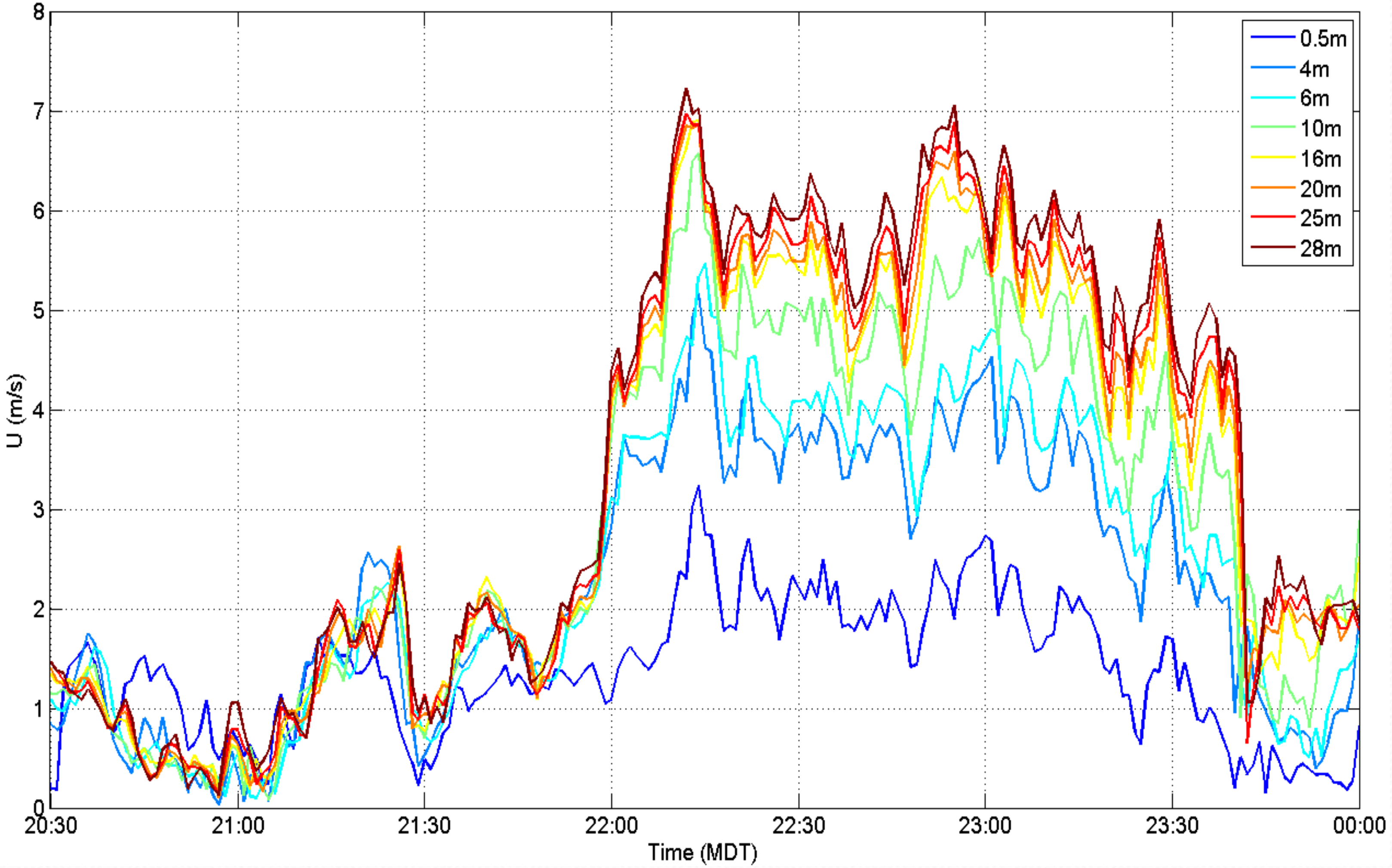

Wind direction at the ES-2 tower (10/19/2012). Prior to 21:00 MDT, the wind direction oscillated due to interacting katabatic and downvalley flow. After the flow developed the wind direction was nearly constant during the measurement period (22:00-23:30 MDT) throughout the height of the tower.

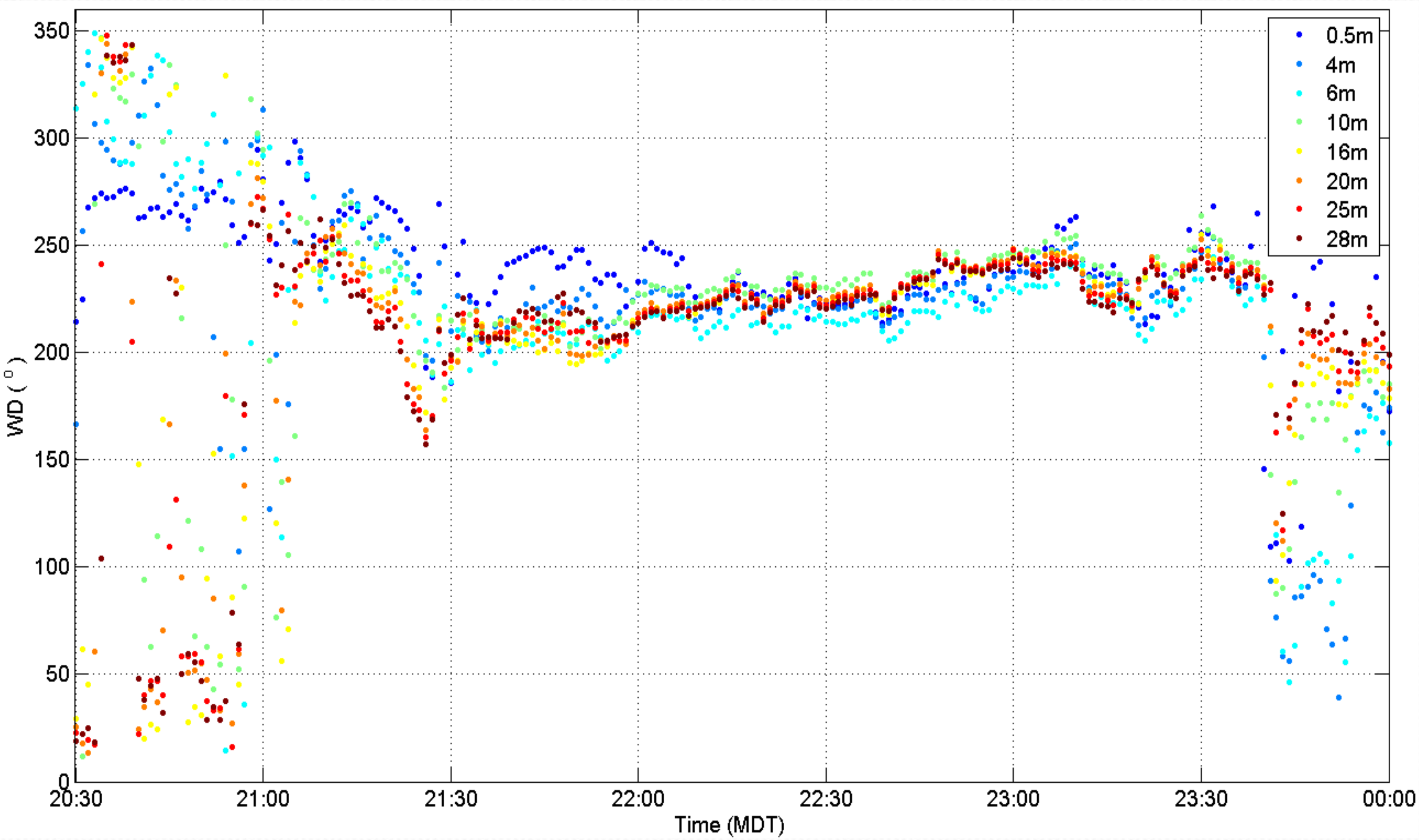

Temperature at ES2 tower (10/19/2012). (Local Utah time: MDT = UTC-6).

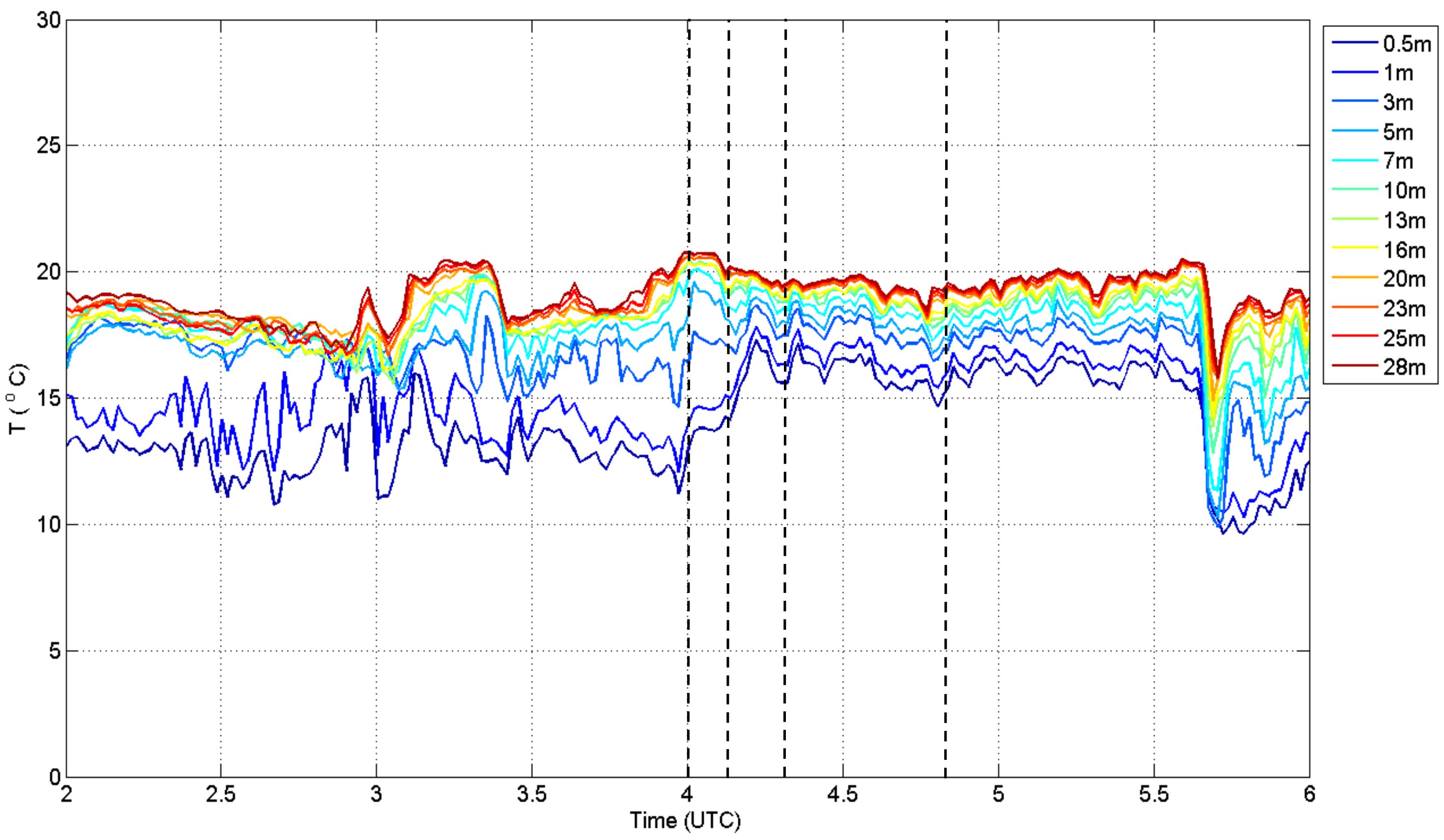

Sonic time series for the nocturnal time period at October 19 (10:00-11:30PM)

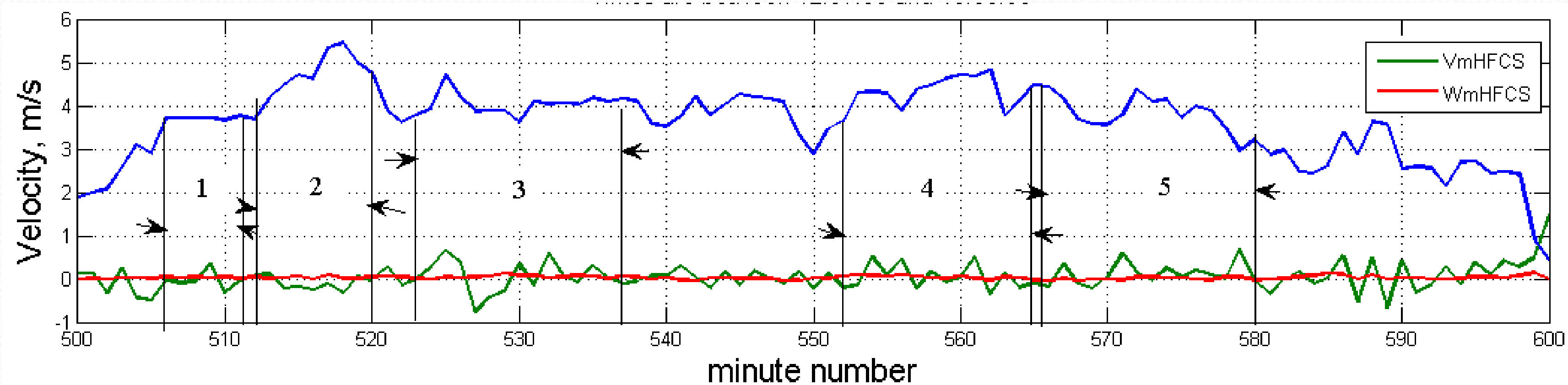

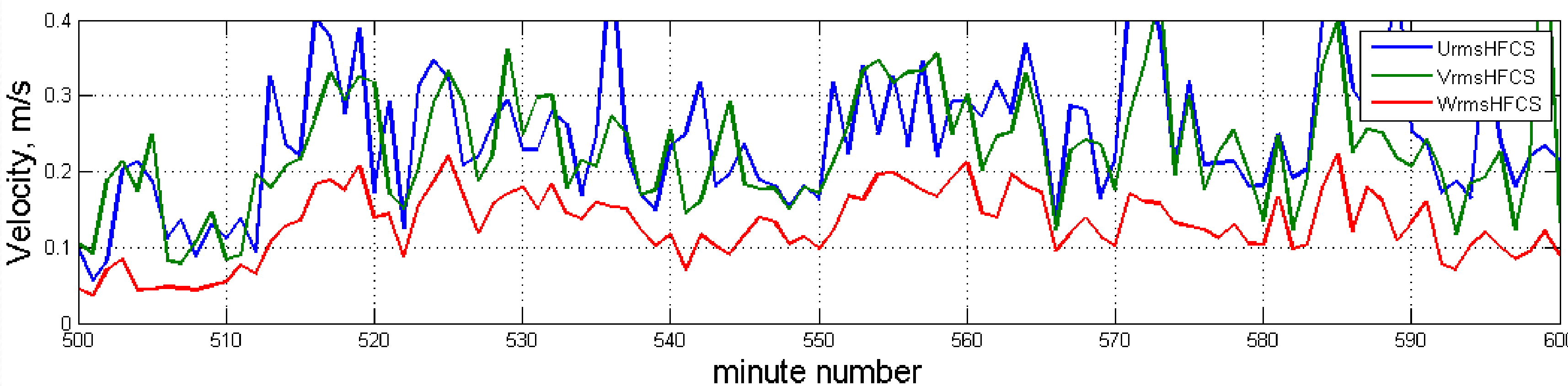

Fourth sub-interval (S-I). Reconstructed velocity field

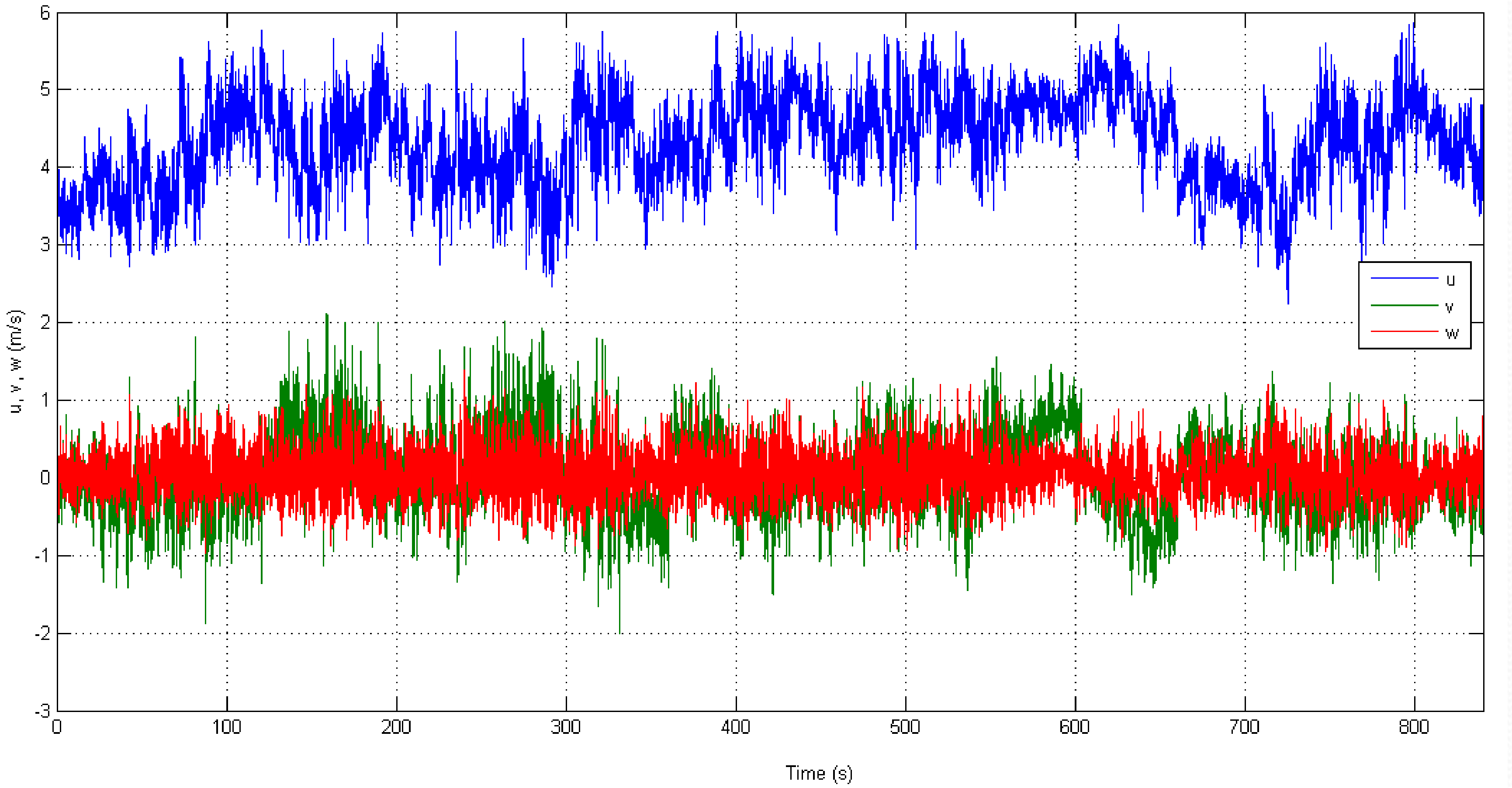

TKE dissipation in 4th S-I

$$\epsilon = 15\nu \overline{\left(\frac{\partial u}{\partial x}\right)^2} \;;\; \partial x = -U\partial t$$

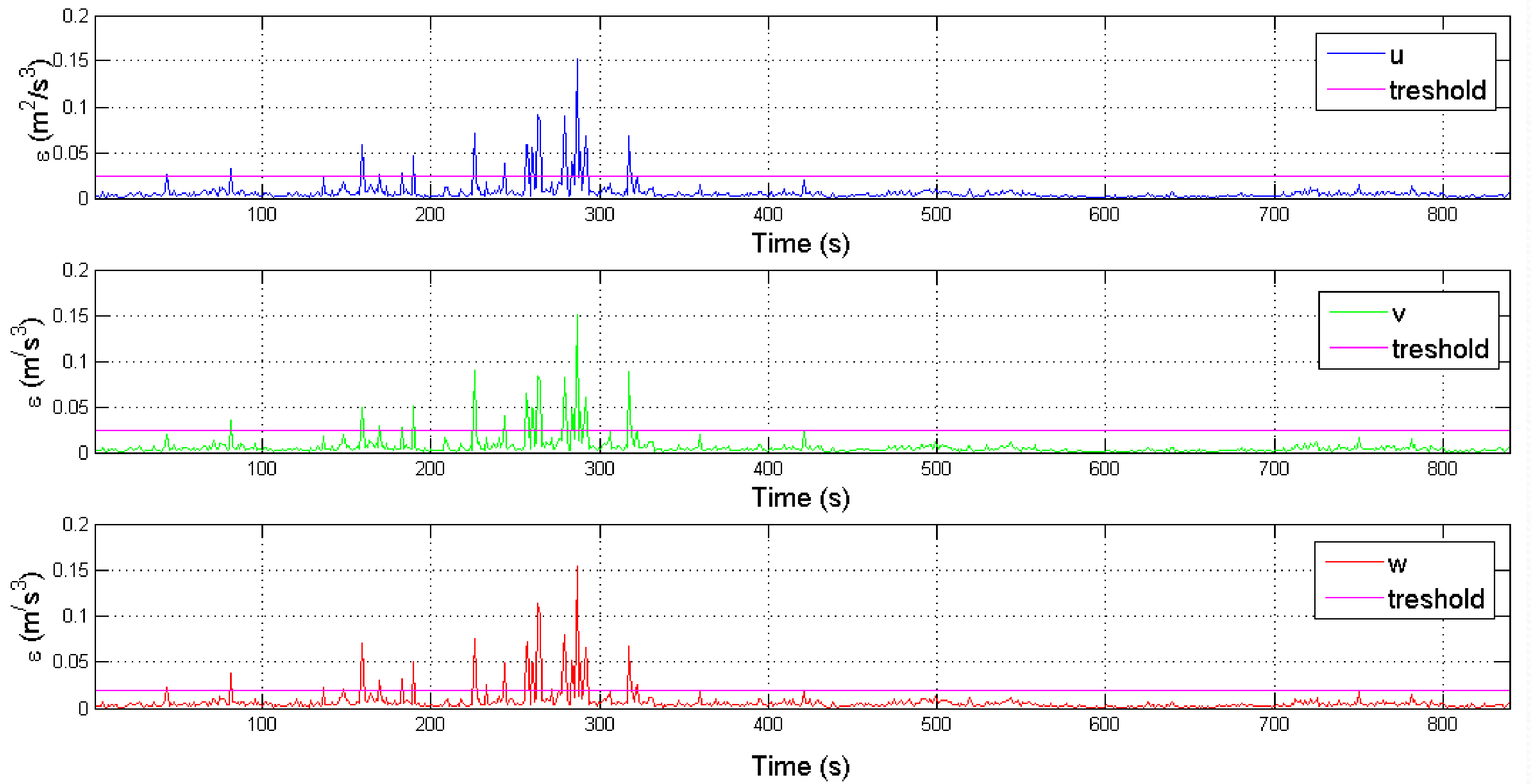

Burst/No-Burst Flag Selection

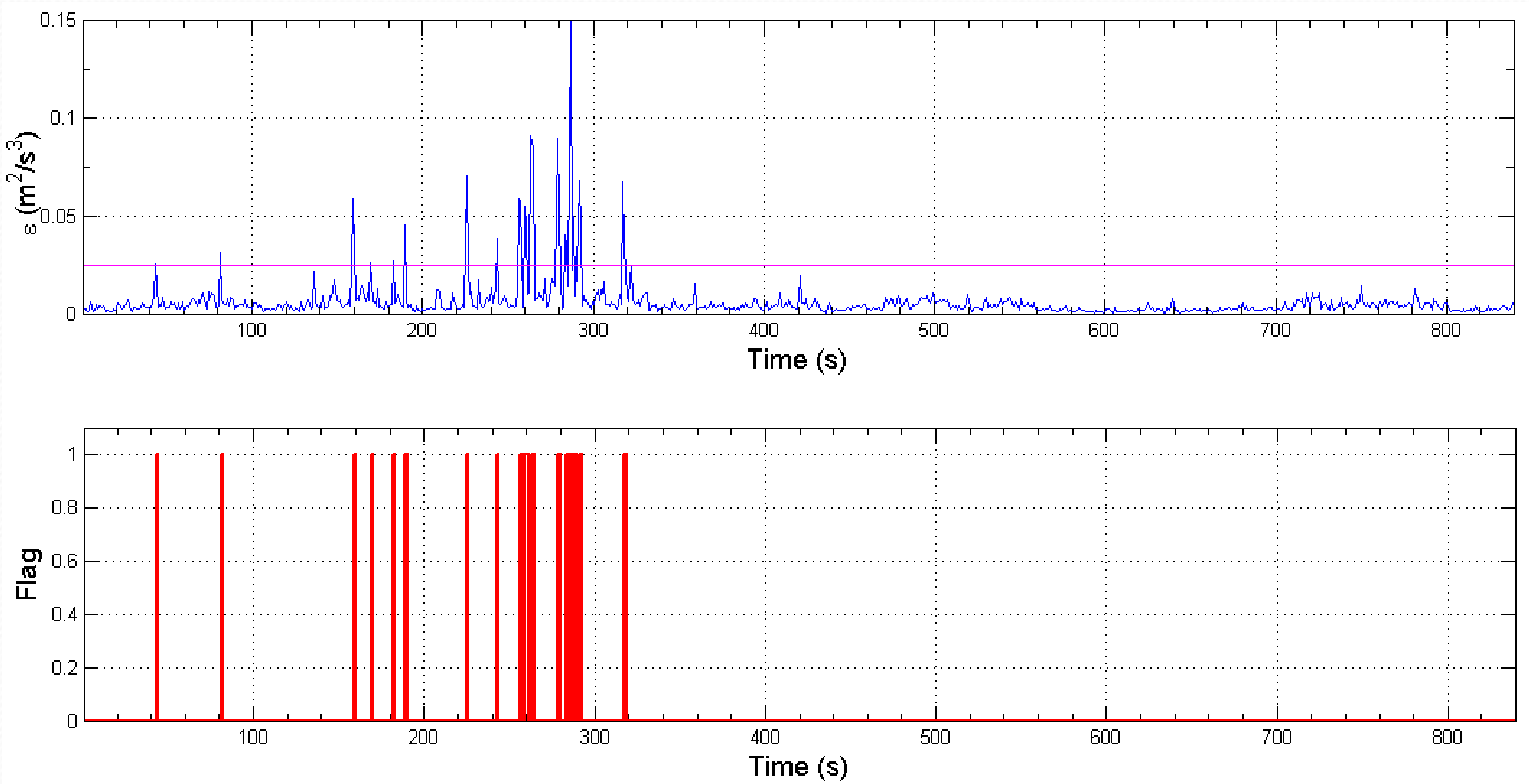

Velocity field at bursting events in forth S-I

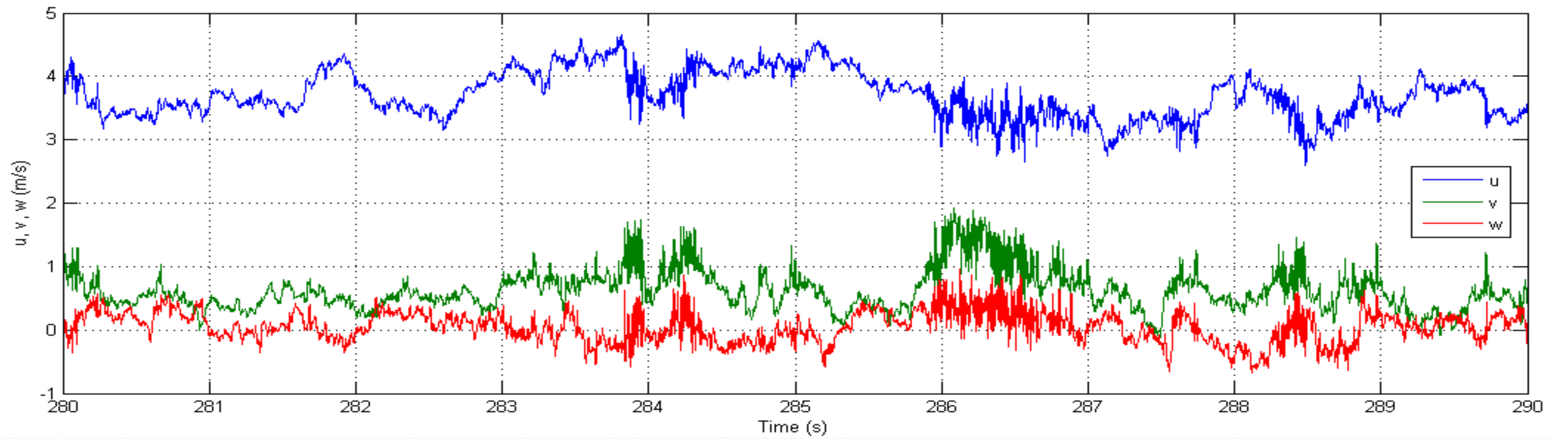

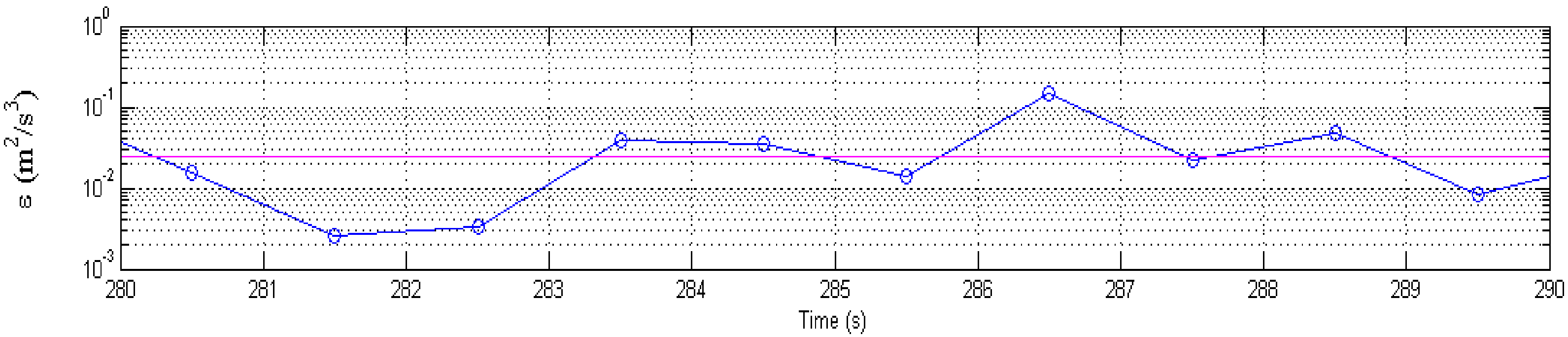

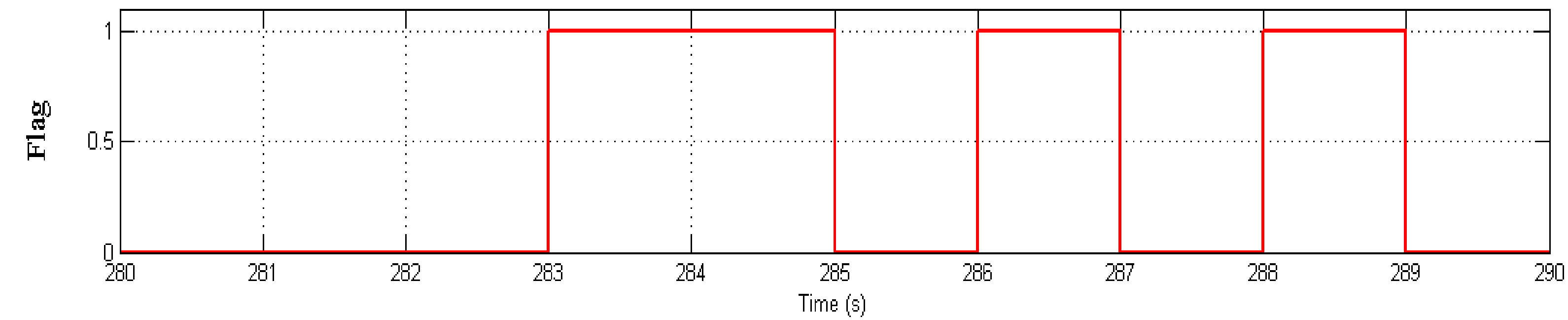

SPECTRA: upper - no-burst, bottom - burst

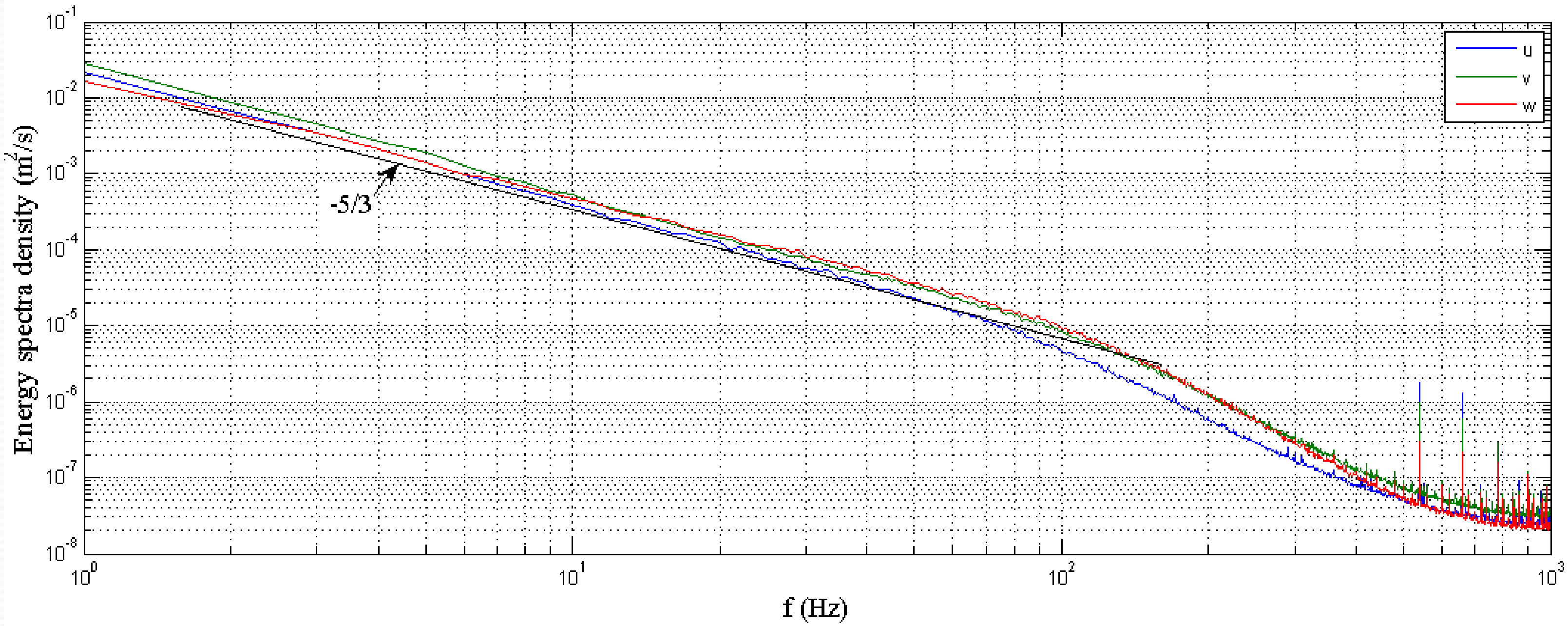

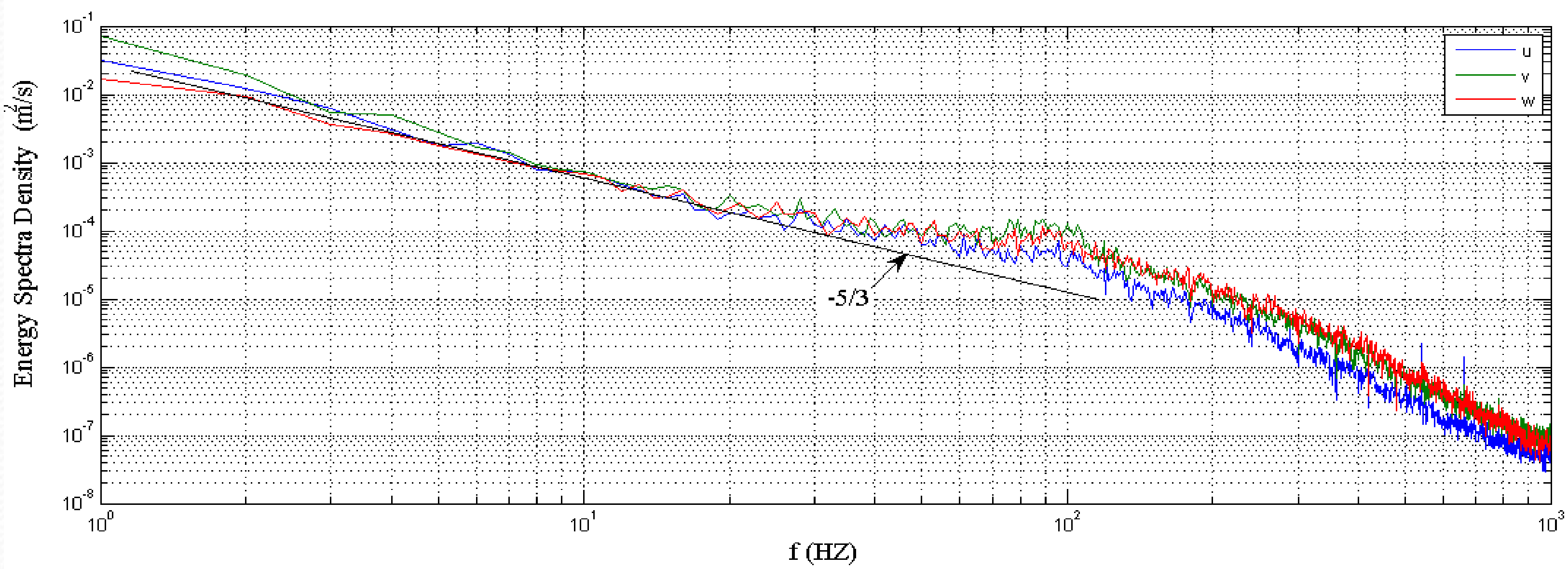

SPECTRA: upper - no-burst, bottom - burst

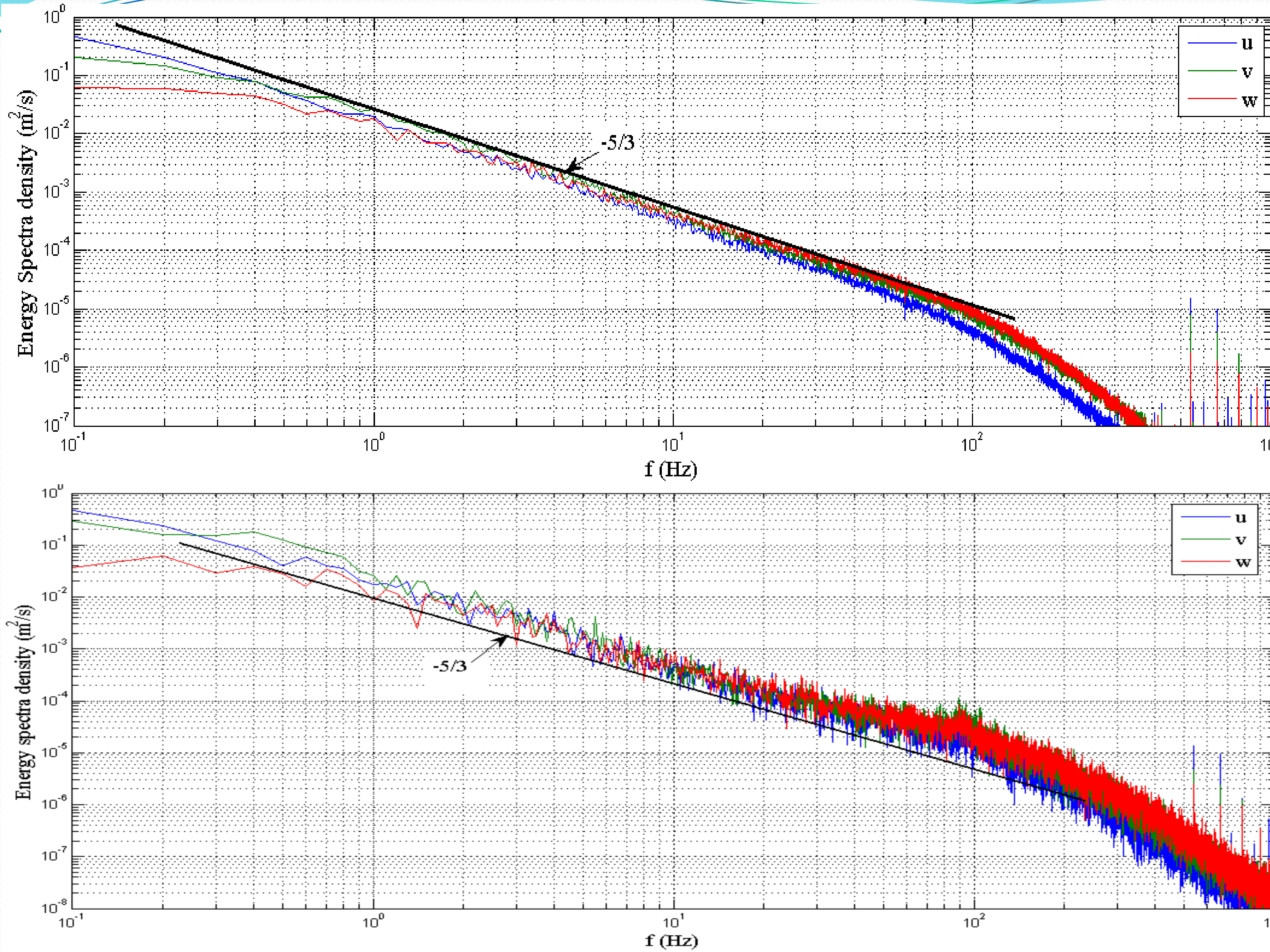

$$S = \overline{(\partial u / \partial x)^3} / (\overline{(\partial u / \partial x)^2})^{3/2}$$

Times series of skewness of the longitudinal velocity derivative

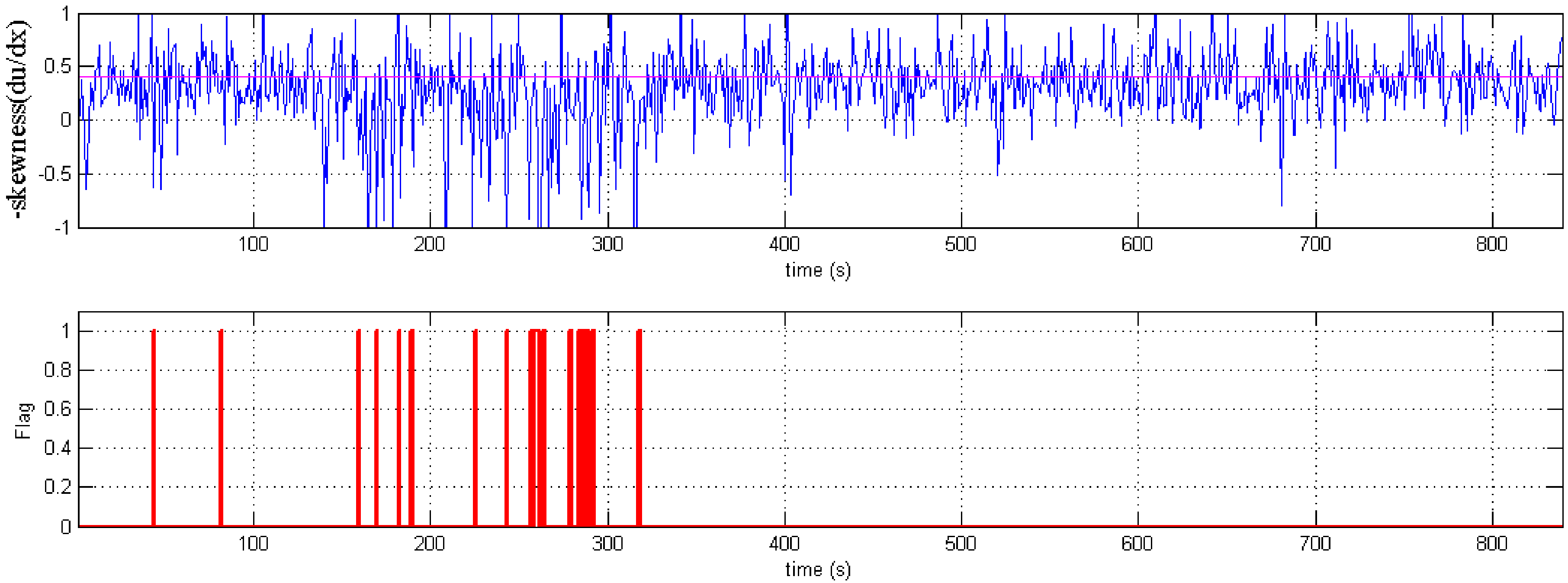

TKE dissipation at 5th S-I and Flag Selection

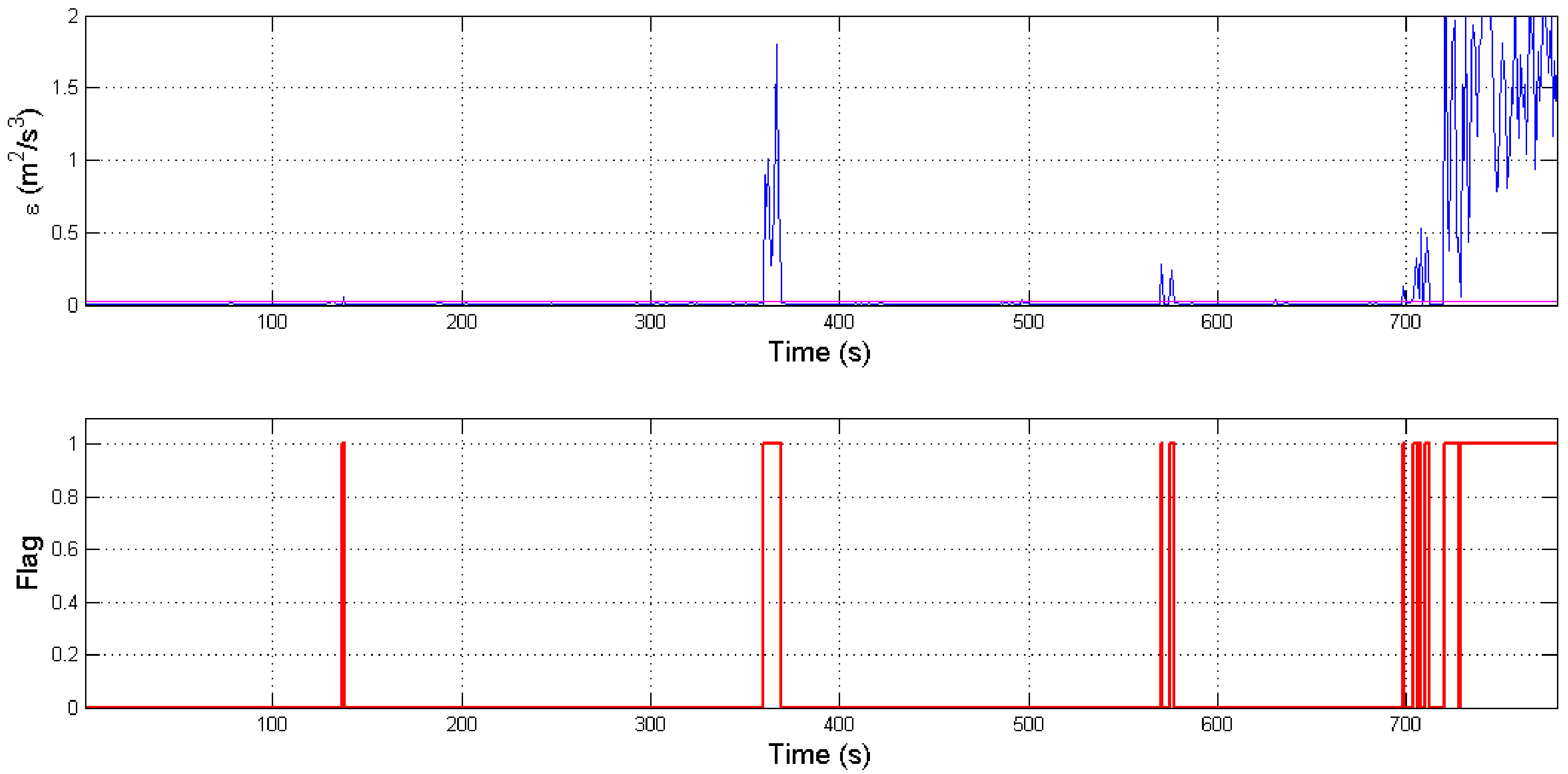

Velocity field at bursting events in fifth S-I

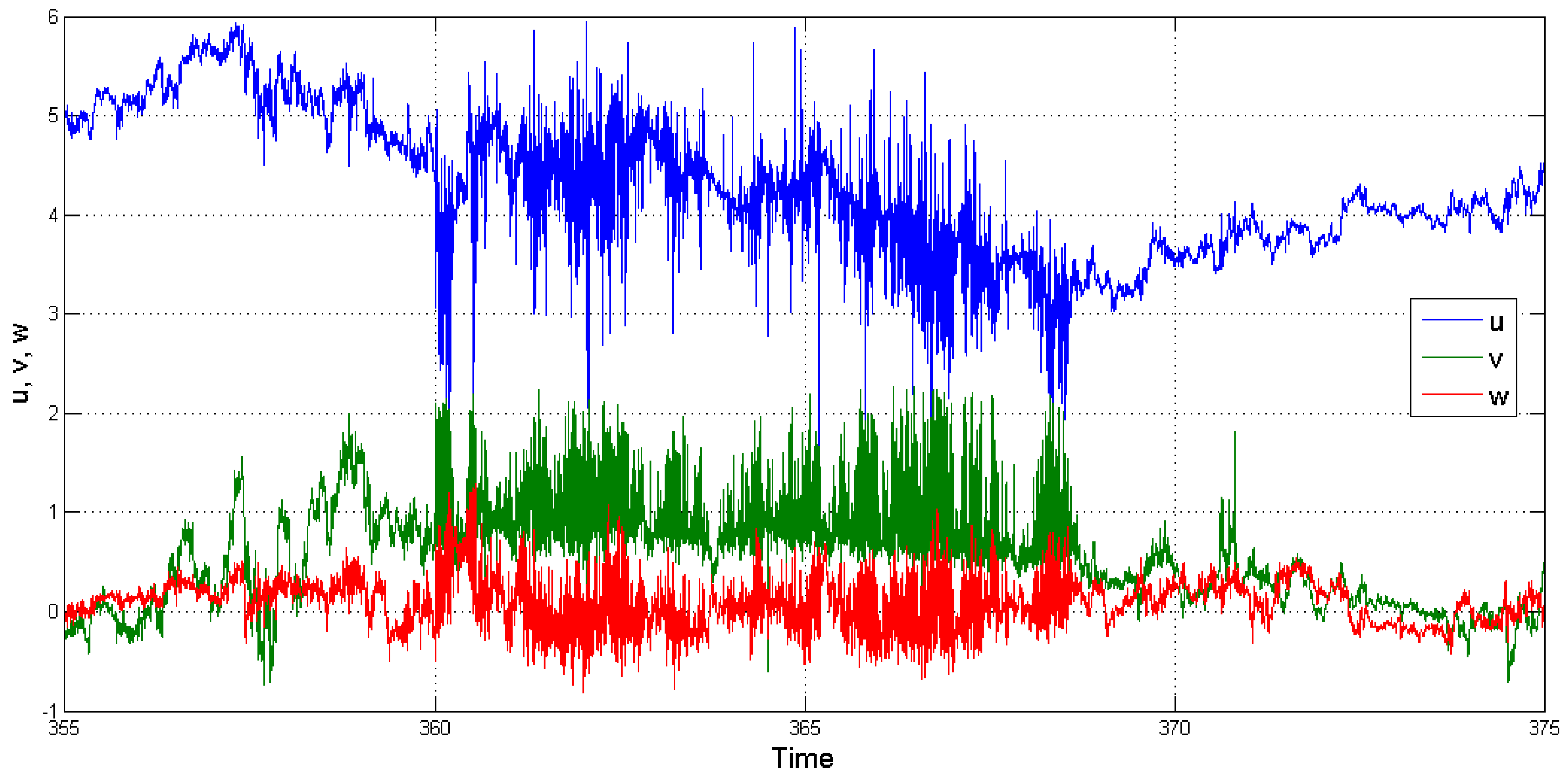

Kolmogorov spectra for non-busting events

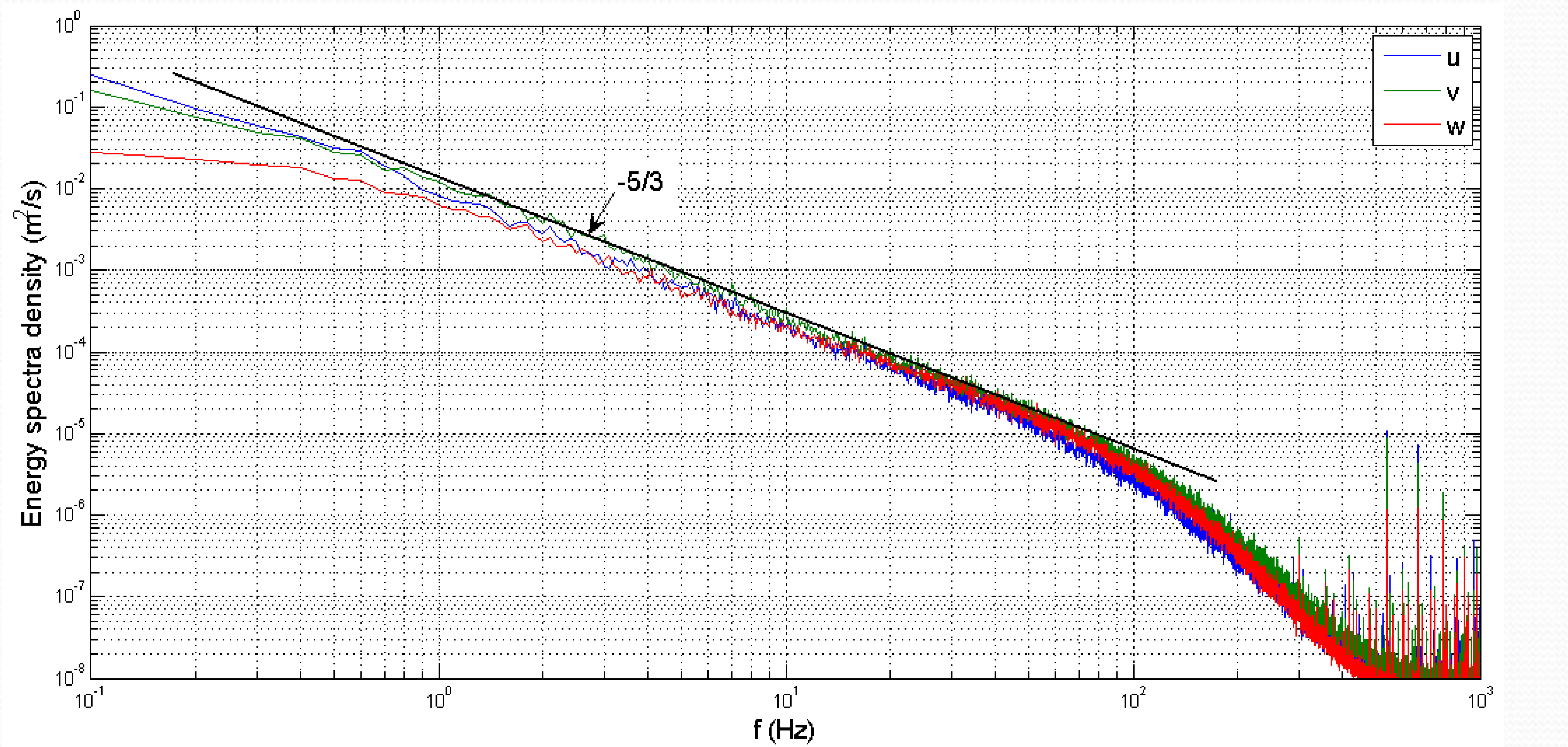

Spectra at busting events

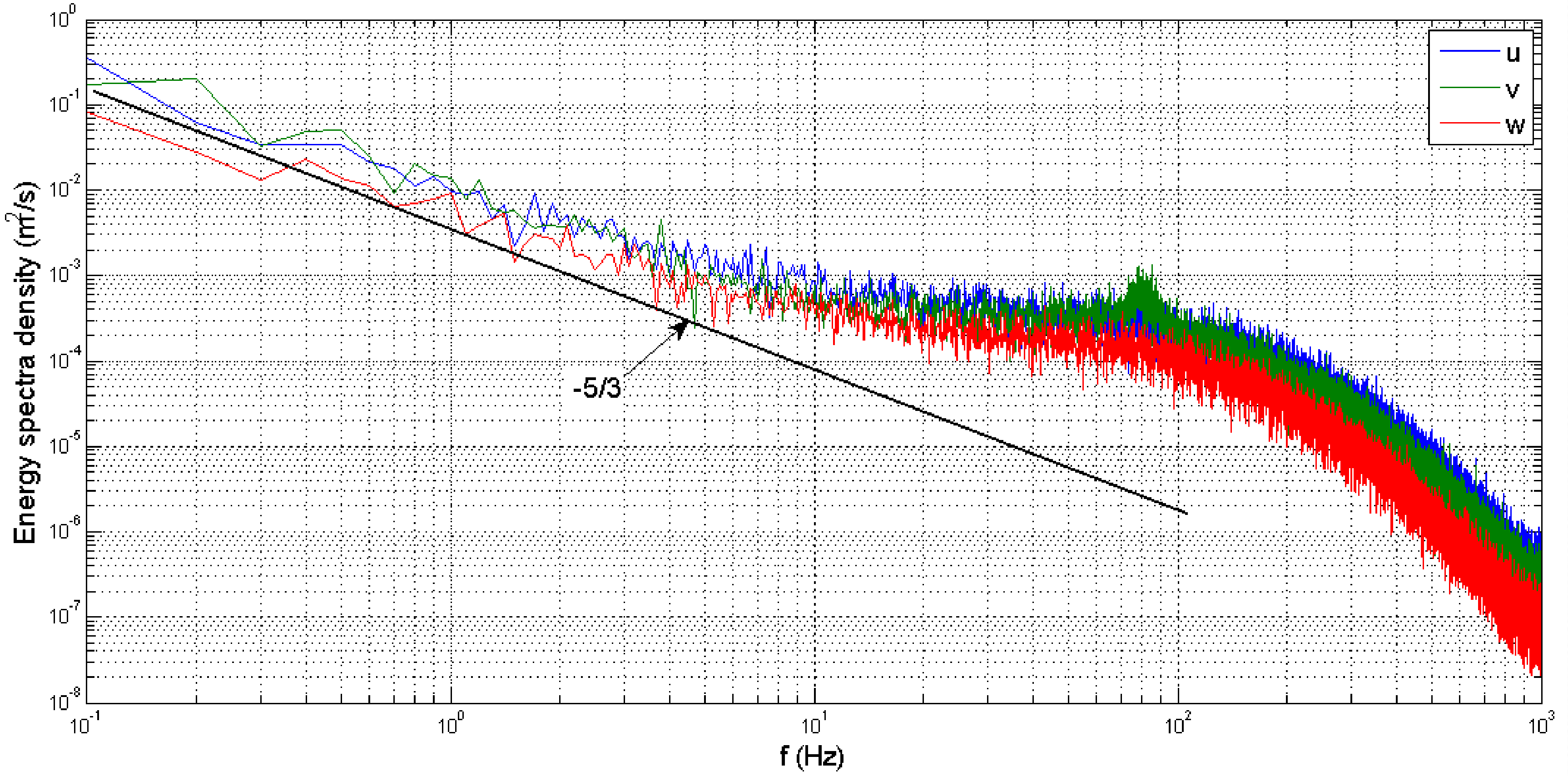

Mean and RMS velocities along with normalized Reynolds stress

Sub-intervals \ Velocities		Time, (s)	U (m/s)	V (m/s)	W (m/s)	σ_u (m/s)	σ_v (m/s)	s_w (m/s)	coruw	Background ε_u (m^2/s^3)
1	No-burst	347	3.71	-0.053	0.034	0.070	0.075	0.050	-0.037	4.1e-4
	Burst	13	3.92	0.533	0.051	0.206	0.234	0.150	0.057	
2	No-burst	195	5.02	-0.201	0.035	0.200	0.187	0.179	-0.241	4.3e-3
	Burst	285	4.684	-0.046	0.006	0.394	0.314	0.303	-0.487	
3	No-burst	494	4.011	-0.238	0.045	0.176	0.192	0.166	-0.194	4.4e-3
	Burst	346	4.132	0.410	0.032	0.343	0.320	0.259	-0.362	
4	No-burst	816	4.338	0.031	0.046	0.207	0.237	0.199	-0.240	4.5e-5
	Burst	24	3.889	0.651	0.038	0.269	0.357	0.235	-0.269	
5	No-burst	702	3.936	0.037	0.005	0.158	0.175	0.133	-0.336	4.5e-3
	Burst	78	3.305	0.220	0.050	0.329	0.323	0.219	-0.257	

Characteristic lengths Scales

- **Ozmidov length scale** $\boldsymbol{L_0 = \sqrt{\varepsilon/N^3}}$
- **Taylor microscale** $L_T = (<(u')^2> / <(\partial u' / \partial x)^2>)^{0.5}$
- **Kolmogorov microscale** $\boldsymbol{L_\eta = (\nu^3/\varepsilon)^{1/4}}$
- Horizontal length scale $L_h = \sigma_u^3/\varepsilon$
- Buoyancy length scale $L_b = \sigma_w/N$
- Shear length scale $L_s = \sigma_u/(\partial U/\partial z)$
- ε is the TKE dissipation rate, ν is kinematic viscosity, N is the Brunt-Väisälä frequency
- (σ_u, σ_w) are the *rms* horizontal and vertical velocity

Time series of length scales during nocturnal transition. (*g*) represents "good" minutes judged by the value of the skewness *S* being in the range of -0.2 > *S* > -0.6 while (*b*) represents "bad" minutes whereas *S* outside of this range.

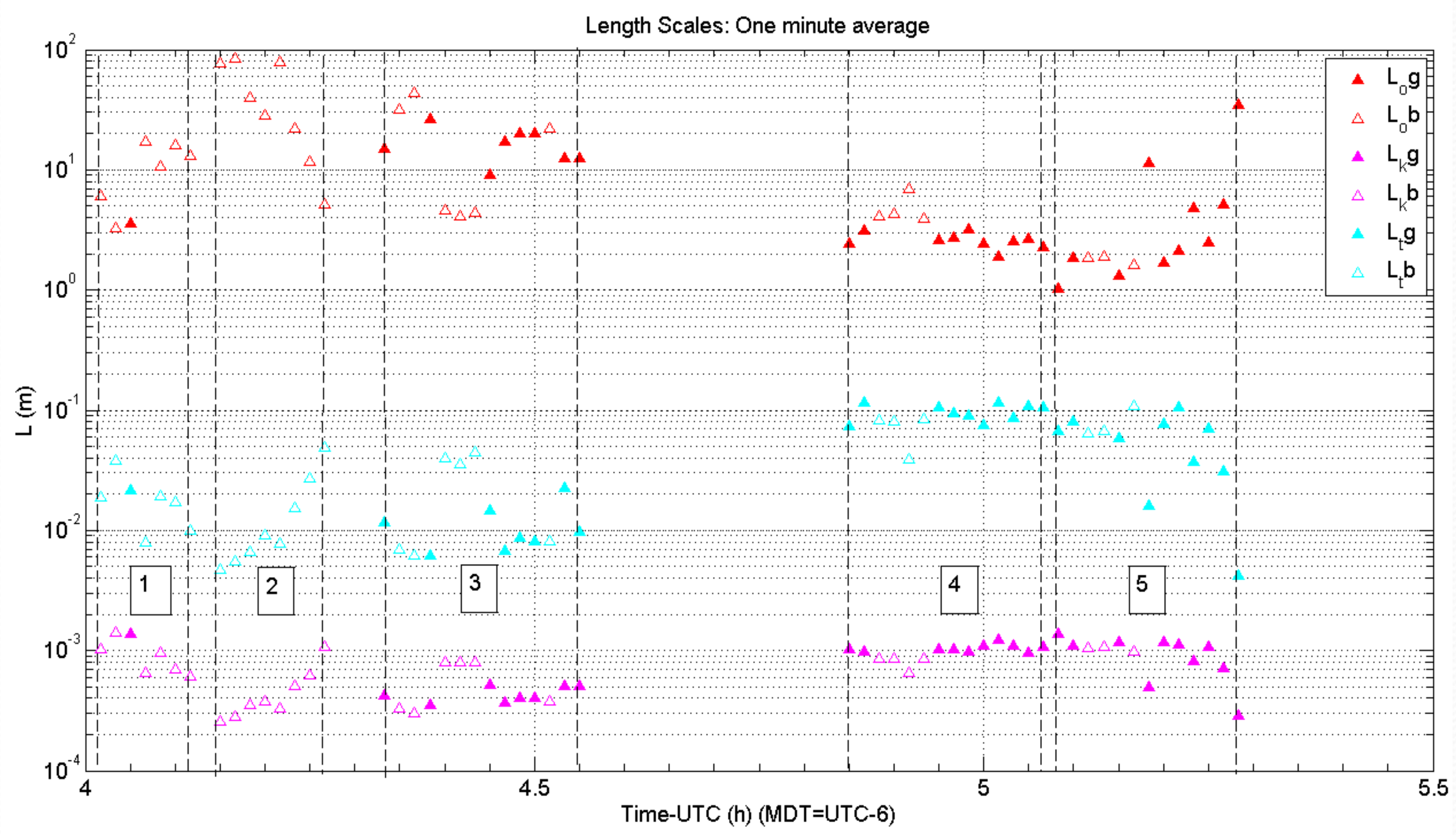

Rig vs. time during the evening transition. In red the selected minute when strong bursts of turbulence were observed. Numbers indicate the sub-intervals

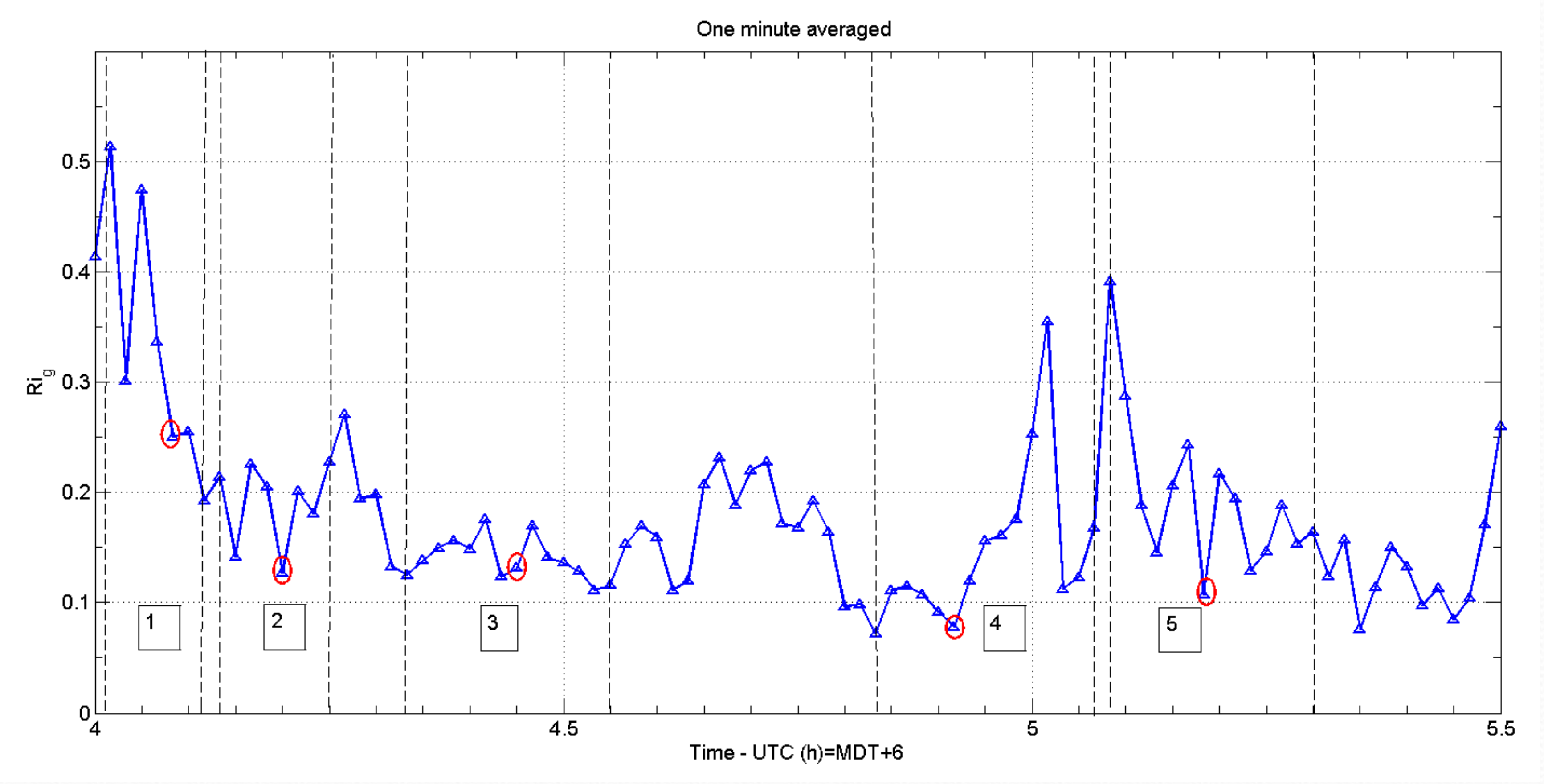

Time histories of w velocity fluctuation and corresponding Richardson umber at z = 30mm, CaseS2. Ohya et al. (2008)

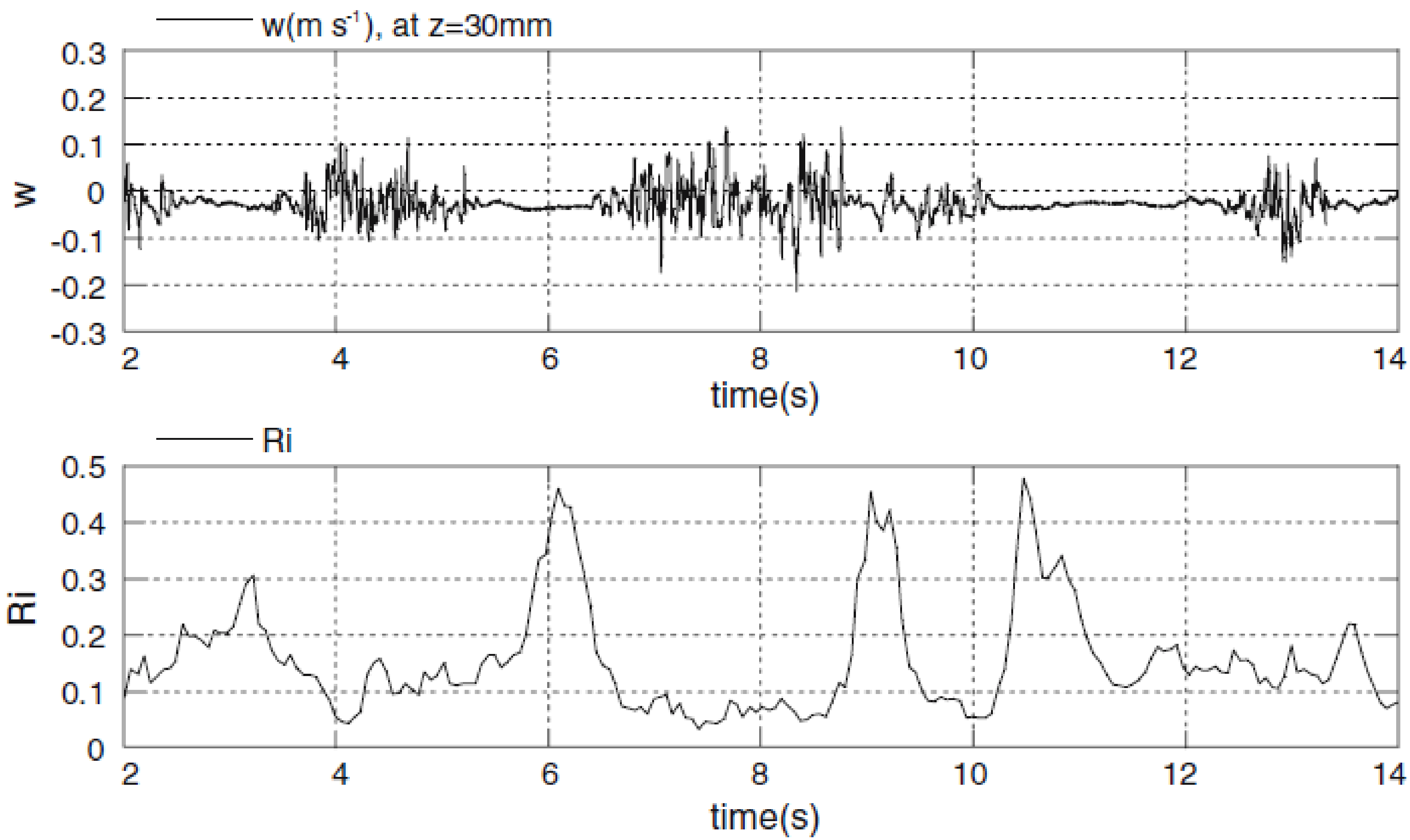

Conclusions

- A combo system consisting of hot-film probes and collocated sonic was developed, with a capability of calibrating the hot-films using ***sonic data and a Neural Network (NN)***.
- A platform was designed to automatically adjust the hot-film probes to the wind direction, prompted by in-situ sonic data.
- An automatic program to collect the data from sonic and hot-film probes enabled to obtain ***continuous data*** without interruption for more than 24 hours.
- In the present study ***90 minutes of superb data*** during an evening transition was measured from an almost laminar flow regime to a fully developed flow regime.
- A new phenomenon was discovered; ***the occurrence of strong bursting of turbulence*** related to the stable stratification.

Continuation…

- Processing procedures were developed for ***separation of the turbulence to burst/no-burst events***.
- The spectra of events without bursting have ***a classical Kolmogorov shape*** while the events with bursting have a ***bumping shape*** resembling ***bottleneck***.
- When the flow is quasi-stationary (e.g. 4th sub-interval), ***skewness of velocity derivative*** oscillates around **-0.4** for the events when the flow does not contain bursts.
- Various lengthscales are presented together with plots of energy spectral density. ***The Ozmidov scale*** separates regions strongly affected by stratification from the region where the classical isotropic Kolmogorov regime took place.
- The distribution of ***the gradient Richardson number*** was presented and qualitative correlation of the observed regimes with these Richardson numbers was suggested.

Continuation…

- Calculations of normalized correlation coefficient between longitudinal and vertical velocity components were performed separately for bursting and non-bursting events. ***Similar values(in the range -0.4 to -0.2)*** were obtained, thus supporting that bursts are related ***to real physics*** and not caused ***by external excitation*** due by noise.
- **There is a strong necessity to continue this research in order to clarify *whether bursting generation* was related to some specific *favorable conditions* in this complicated mountain terrain or represents *a generic phenomenon* that occurs due to strong stratification during evening periods. The answer to this question is of great importance for developing a more complete understanding of atmospheric boundary layers in mountainous terrain regions.**

THANK YOU!
THE END

Three velocity components in a bursting event are shown for the end of fourth minute of the first sub-interval. Record duration of 10 sec is presented.

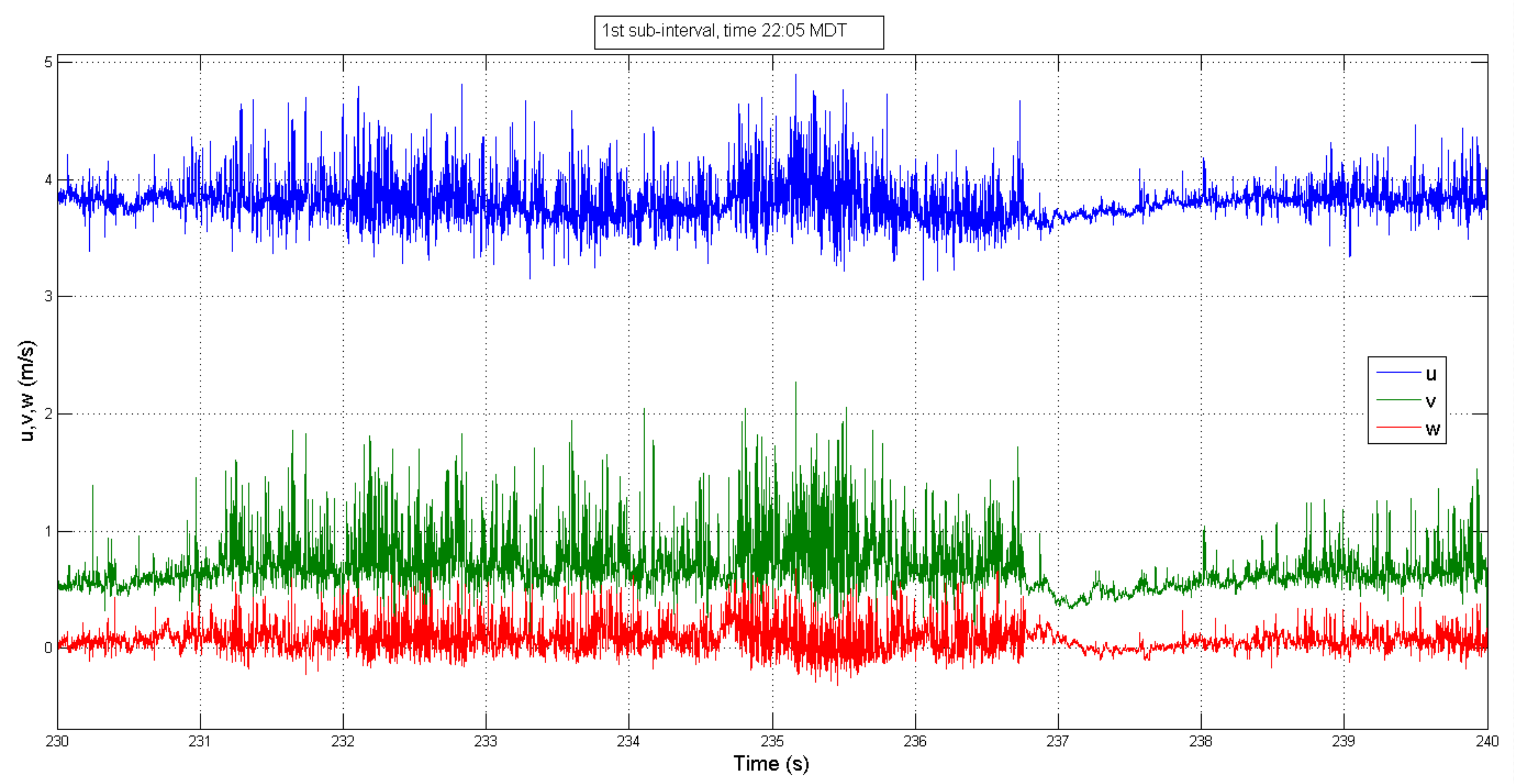

Three velocity components in a bursting event are shown for the beginning of fifth minute of the second sub-interval. Record duration of 10 sec is presented.

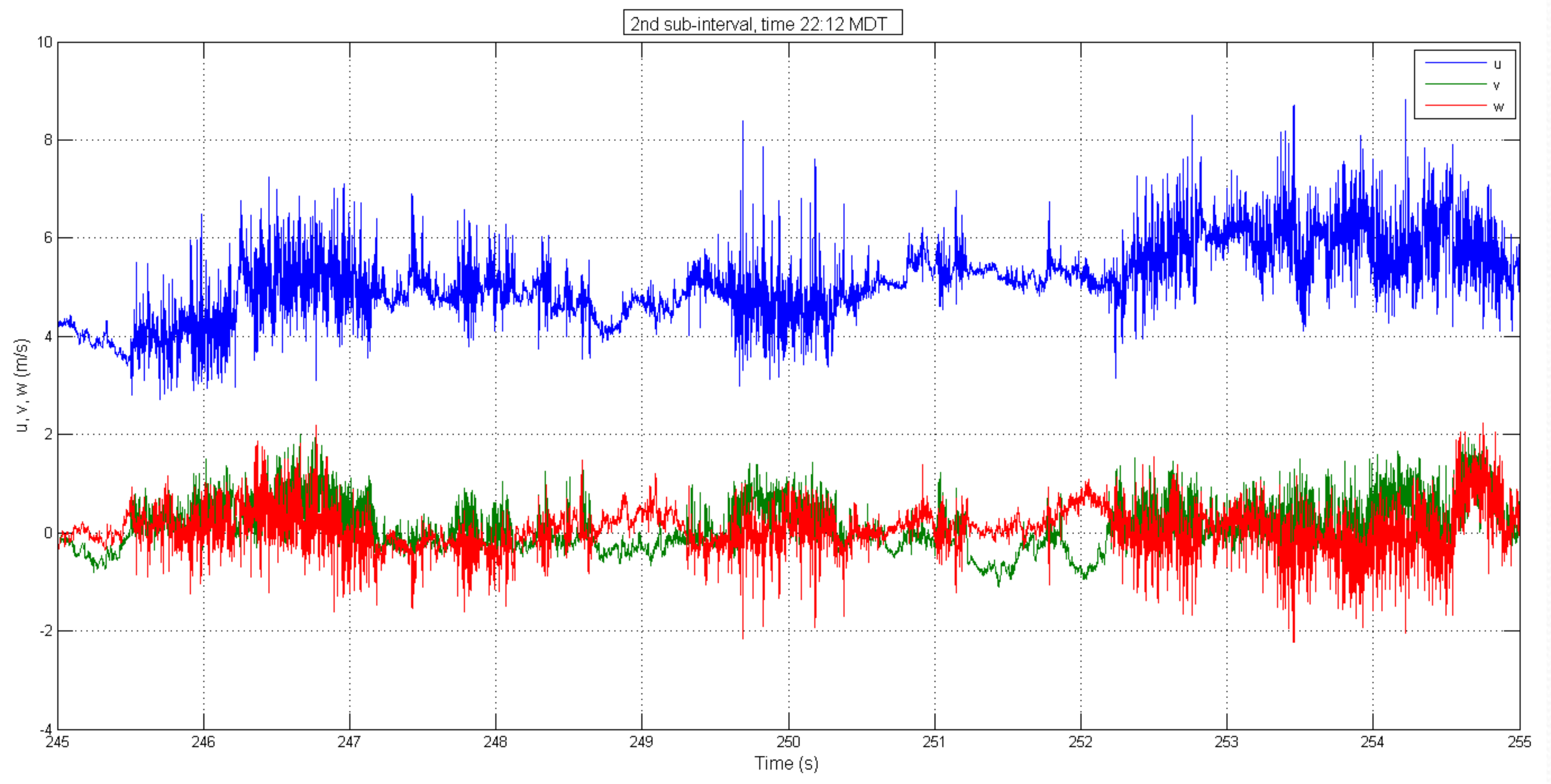

Three velocity components in a bursting event are shown for the beginning of sixth minute of the third sub-interval. Record duration of 10 sec is presented

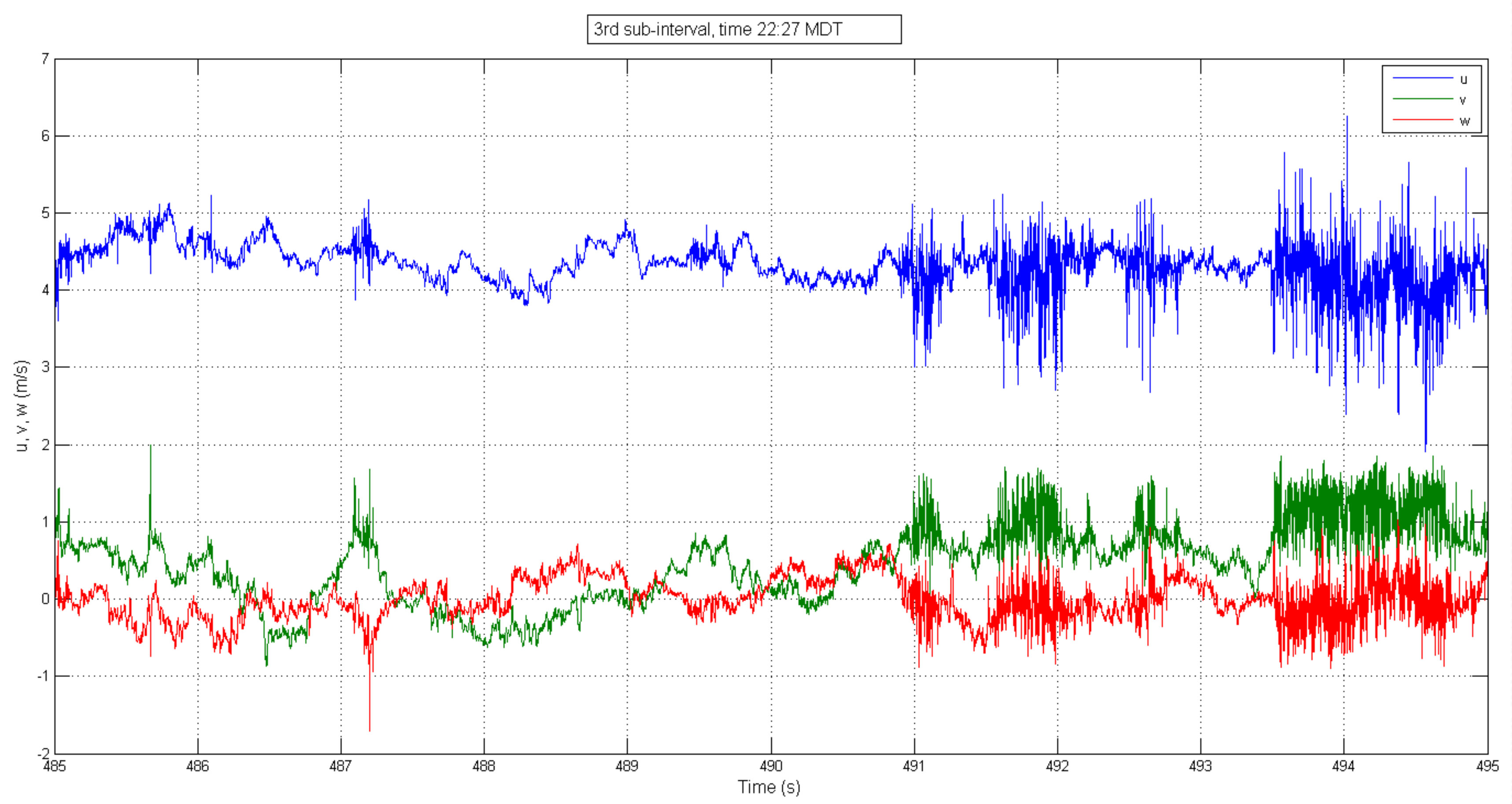

Three velocity components in a bursting event are shown for the end of fifth minute of the fourth sub-interval. Record duration of 10 sec is presented

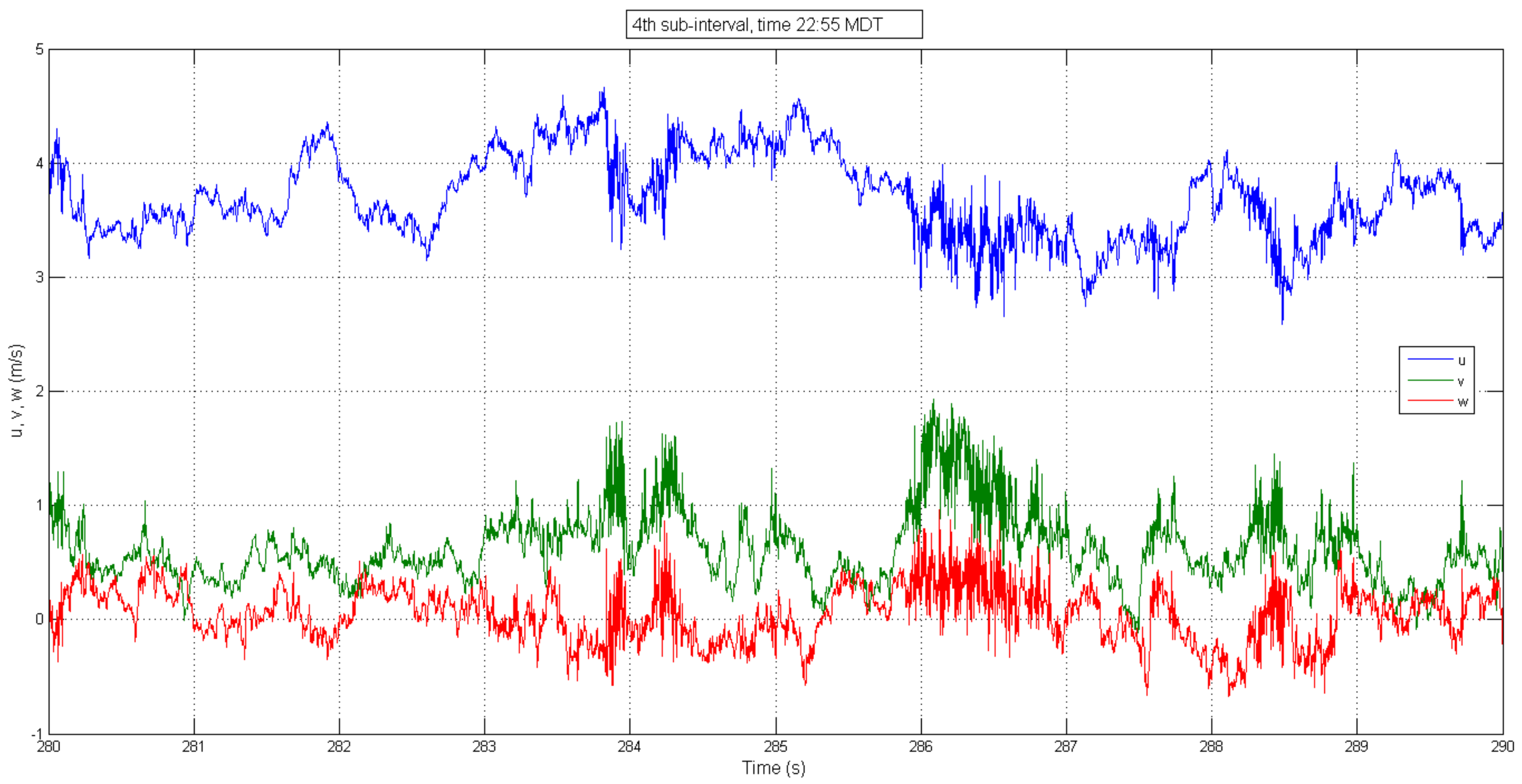

Three velocity components in a bursting event are shown for the end of sixth and beginning of seventh minutes of the fourth sub-interval. Record duration of 10 sec is presented

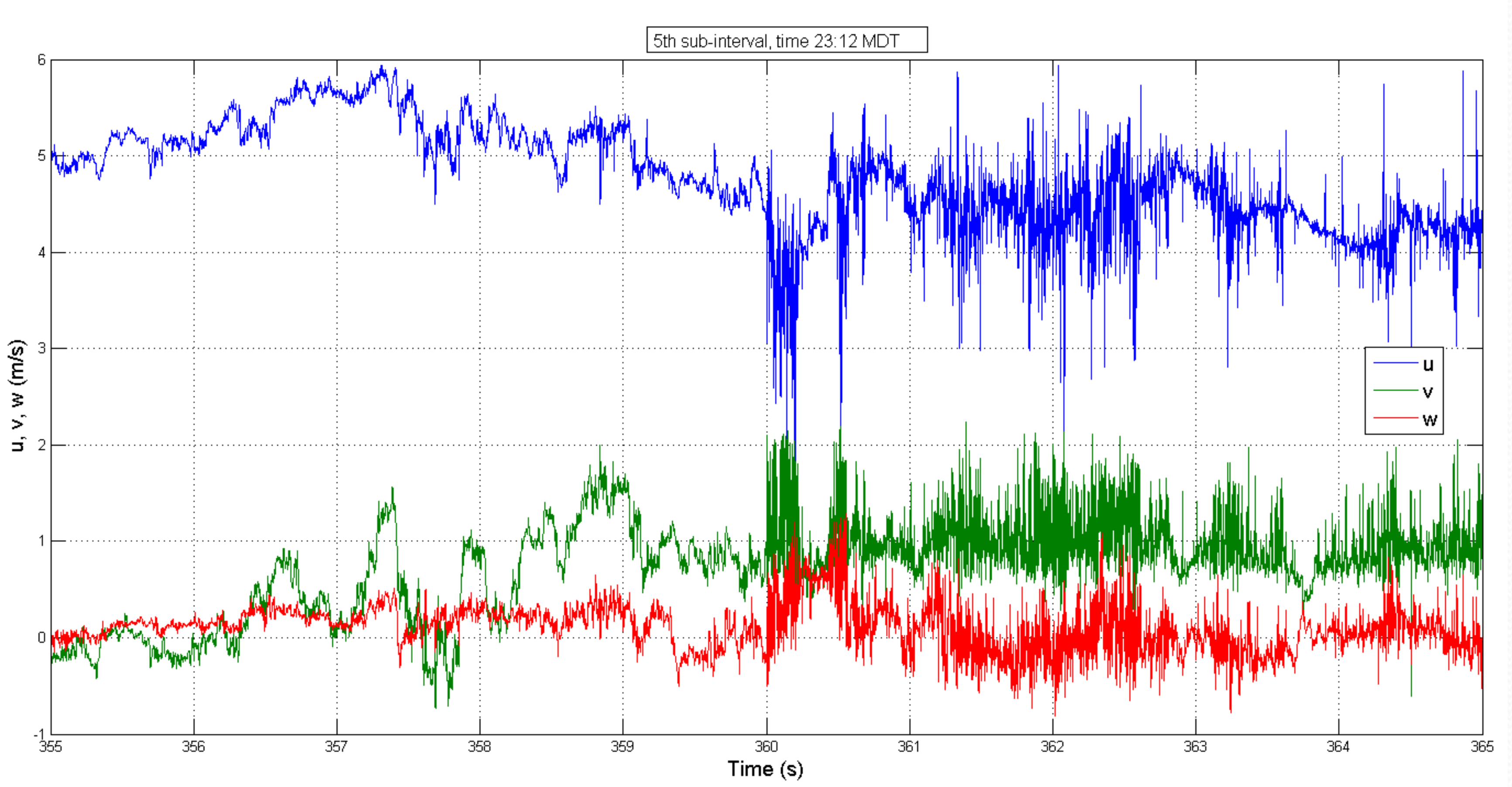

Flow visualization in laboratory experiments by Ohya (2001): top, middle and bottom plates are neutrally, weakly and strongly stratified BLs, respectively.	Flow visualization of SBL with a low-level jet, side view (Ohya et al. 2008, Case S2). Flow is left to right. Turbulent bursts and downward propagating turbulent puffs produced by a shear layer breakdown are clearly identified.

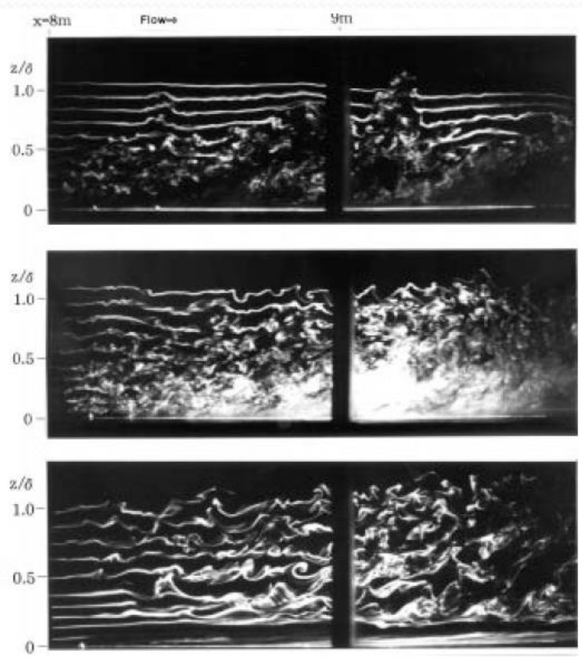

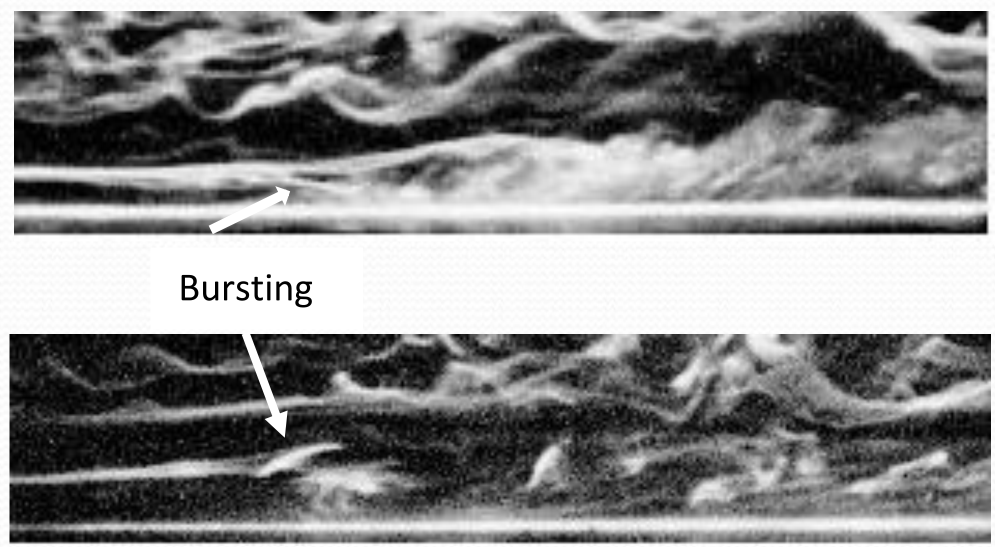

Time series of the longitudinal (*u*) velocity fluctuations in the laboratory experiments by Ohya et al. (2008), Case S2, showing a sequence of strong bursts

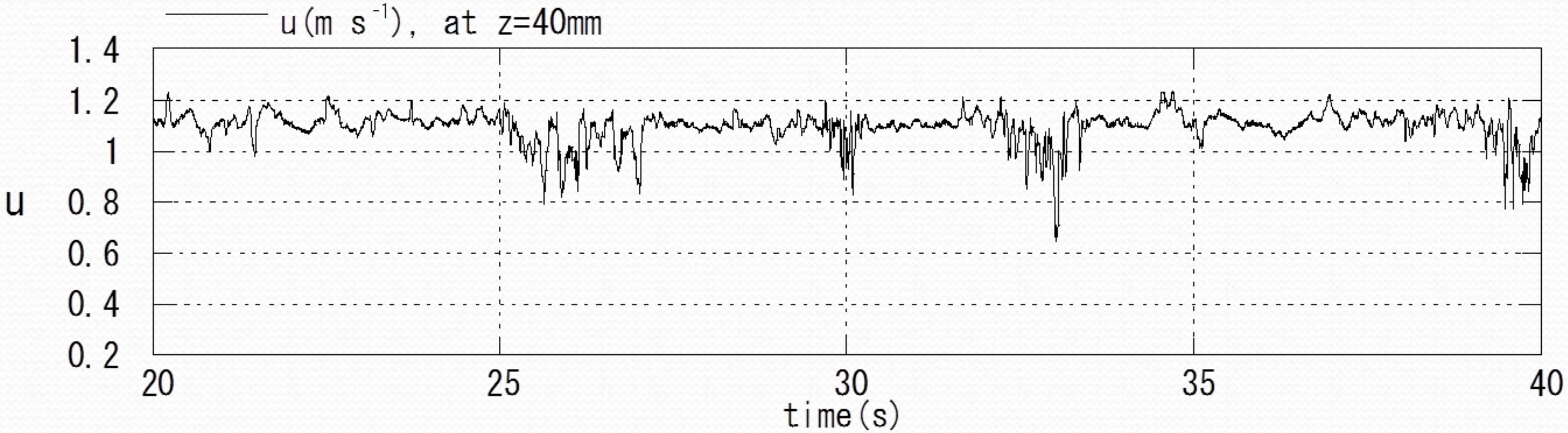

NEW HARDWARE DEVELOPMENTS

New supports for hit-film multi-sensors

4-wire array home-made and used by Tsinober, Kit and Dracos (JFM, 1992)

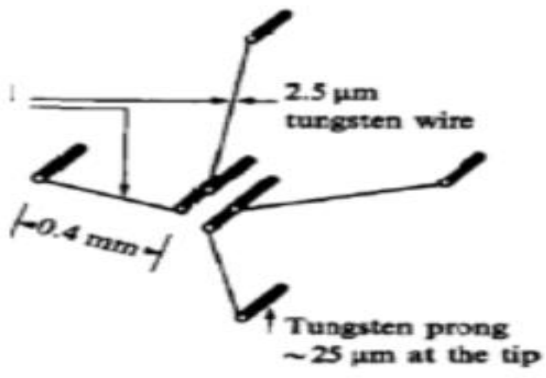

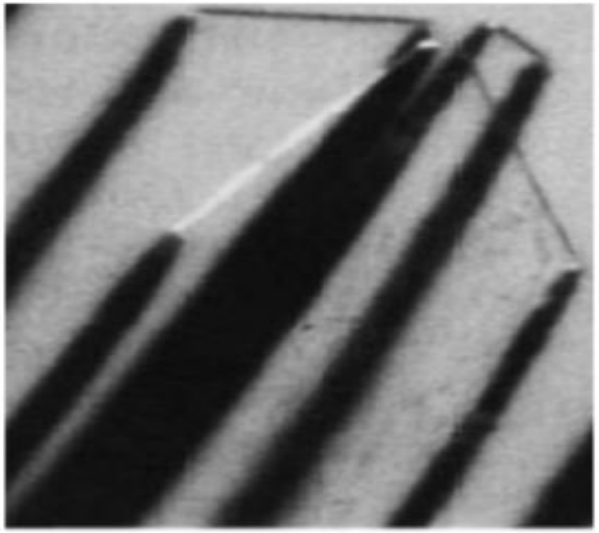

DANTEC Development of a new 3D-probe with 4 hot-film sensors.

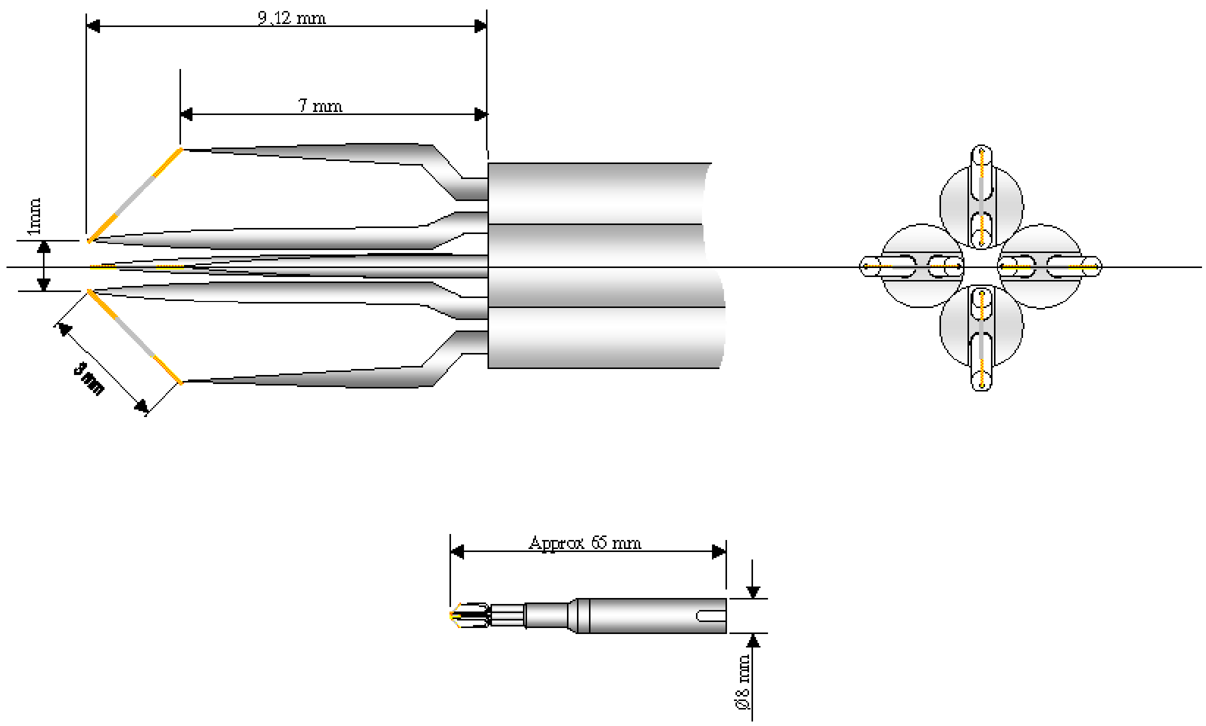

Relevant Papers

- E. Kit, A. Cherkassky, T. Sant, H.J.S. Fernando. *In-situ* calibration of hot-film probes using a co-located sonic anemometer: Implementation of a neural network. **Journal of Atmospheric and Oceanic Technology-AMS, Vol. 27**, No. 1, 23-41 (2010).
- E. Kit and B. Gritz. *In-situ* calibration of hot-film probes using a co-located sonic anemometer: angular probability distribution properties. **Journal of Atmospheric and Oceanic Technology-AMS, Vol. 28**, 104-110 (2011).
- L. Vitkin, D. Liberzon, B. Grits and E. Kit. Study of *in-situ* calibration performance of co-located multi-sensor Hot-Film and Sonic anemometers using a "virtual probe" algorithm. **Measurement Science and Technology 25**, 075801 (2014) doi:10.1088/0957-0233/25/7/075801.

Presentation of velocity components as polynomials of voltages across the wires.
TKE dissipations and skewness of velocity derivatives

$$U_i = f_i(E_1, E_2)$$

$$f_i(E_1, E_2) = \sum_{kl} c_{ikl} P_k(E_1) P_l(E_2); \;\; P_k(E) = E^k, 0 \le k, l \le 4, k + l \le 4$$

Linear system for determination of polynomial coefficients *c* is obtained from calibration data using the least square fit.

Dissipation: $$\epsilon = 15\nu \overline{\left(\frac{\partial u}{\partial x}\right)^2} \; ; \;\; \partial x = -U \partial t$$

Skewness of velocity derivative: Sk= $\overline{\left(\frac{\partial u}{\partial x}\right)^3} / \left(\overline{\left(\frac{\partial u}{\partial x}\right)^2}\right)^{3/2}$

Combo in the Lab

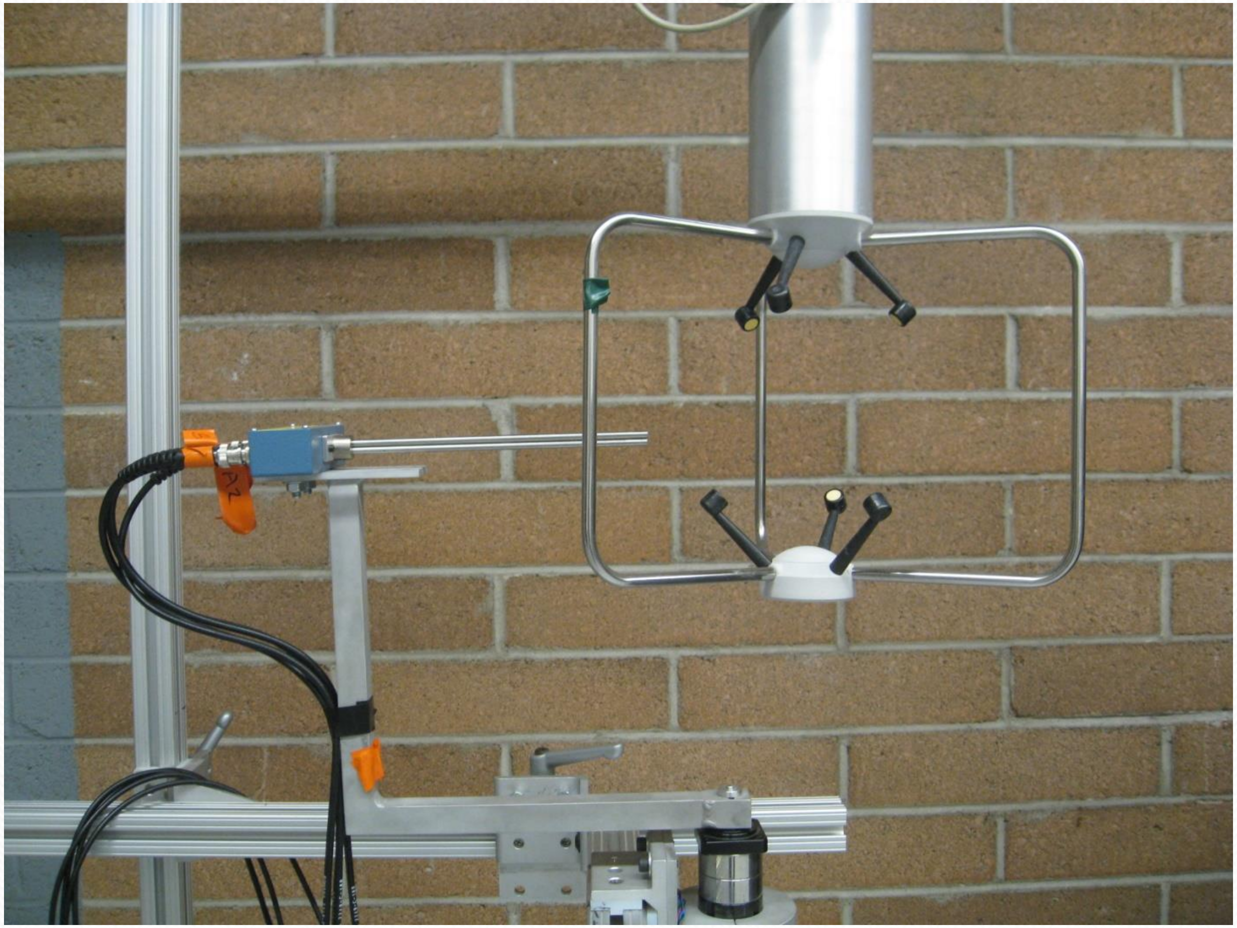

Neural Network

The structure of the generated neural network (3-layer Perceptron)

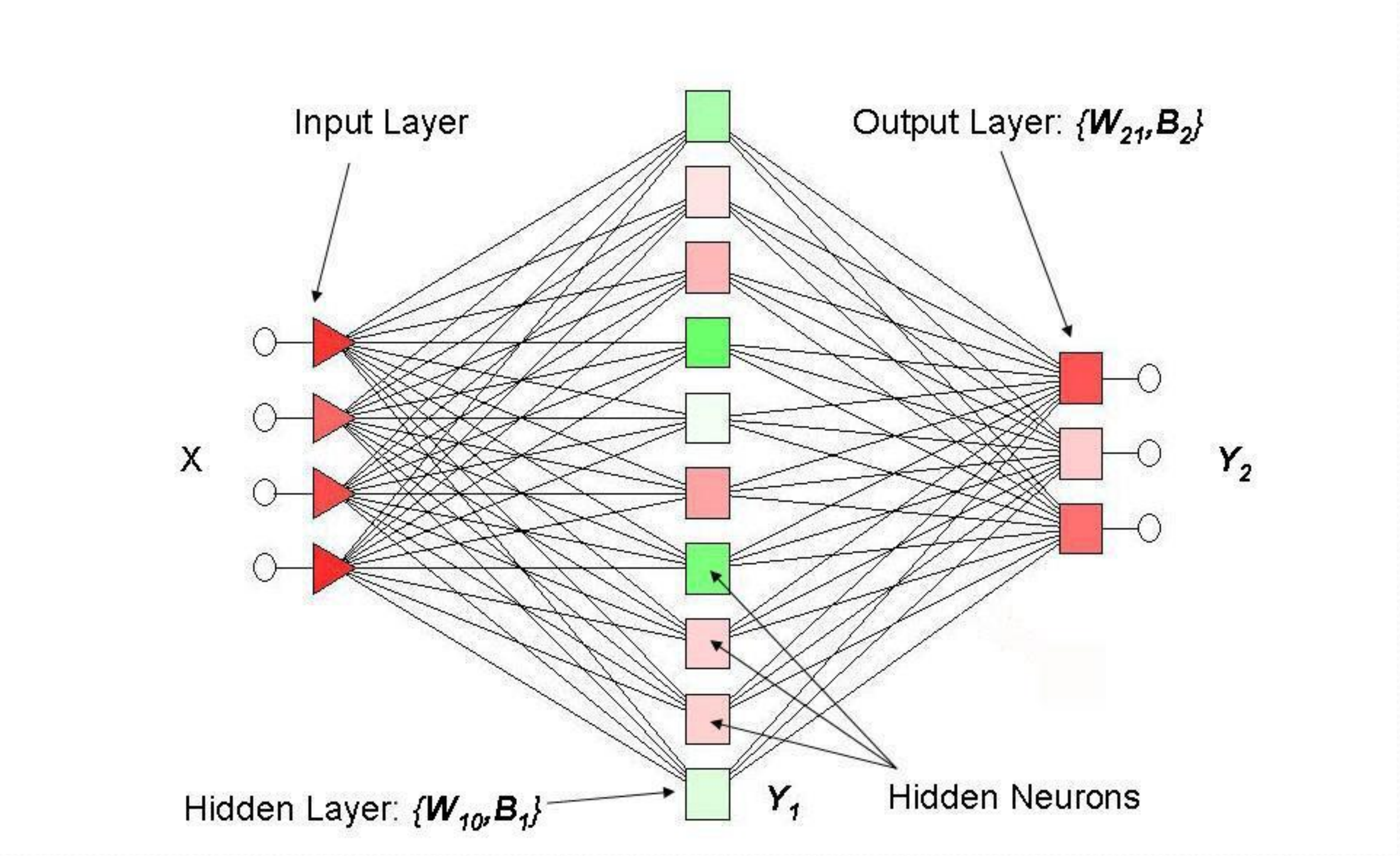

Neural Network Training using MATLAB

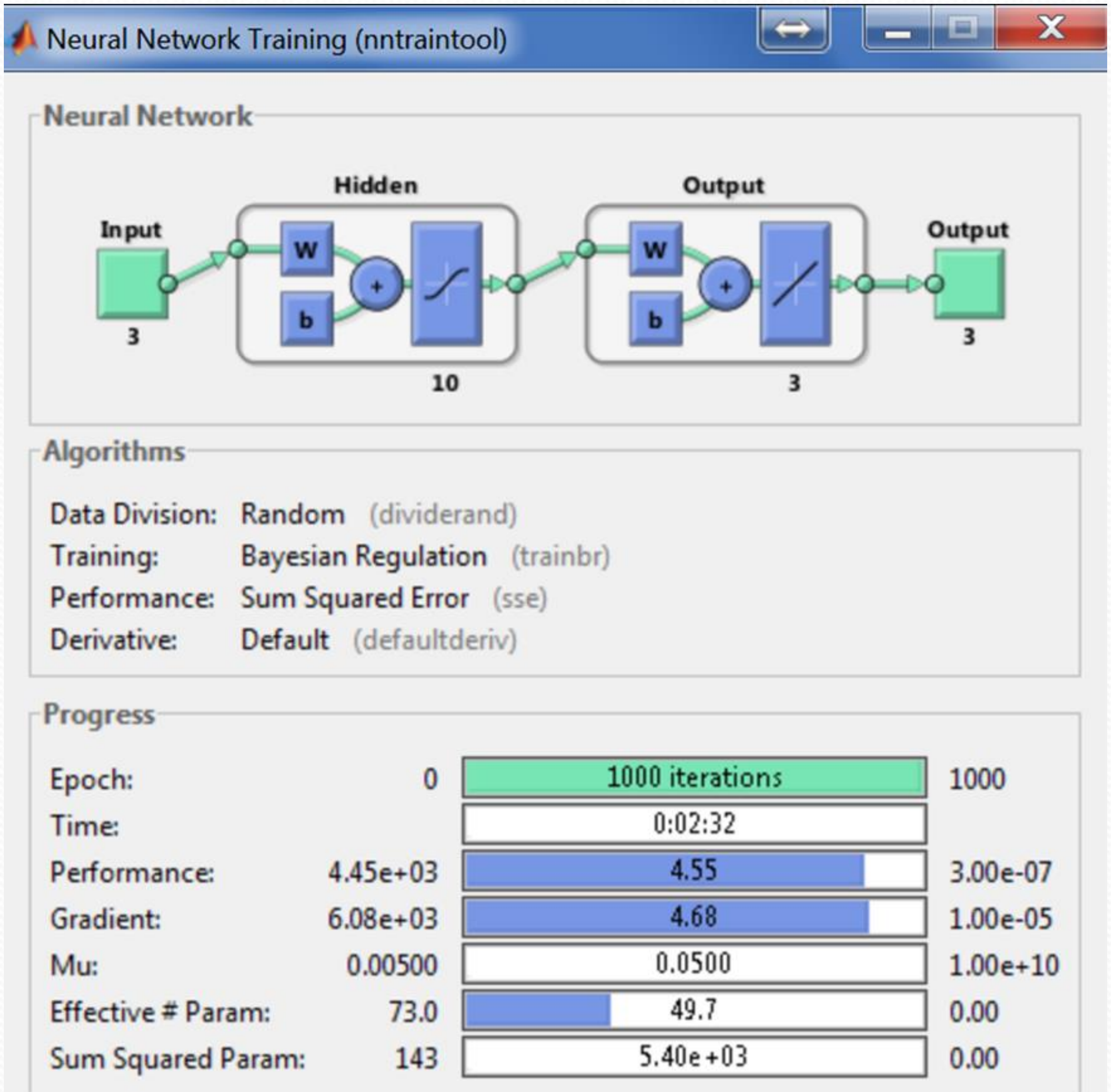

Combo probe Setup: (A) During the initial set-up (2&6m) (B) Second Half (both combos at 6m)

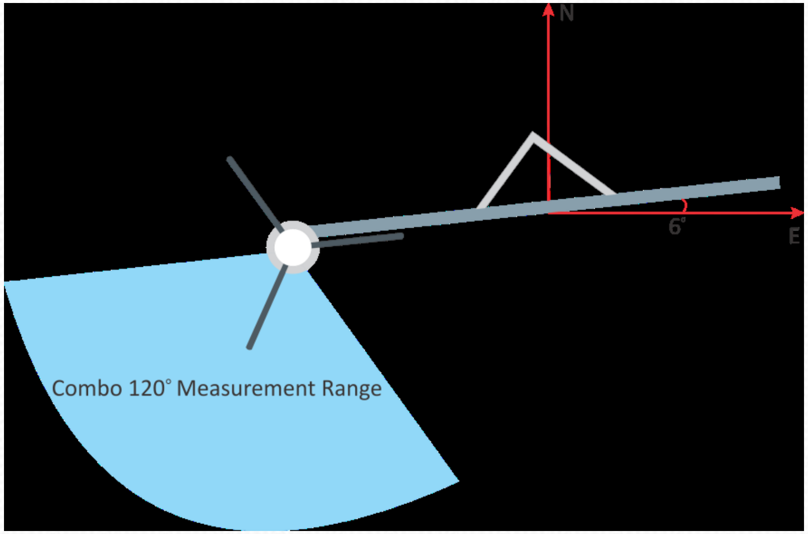

A

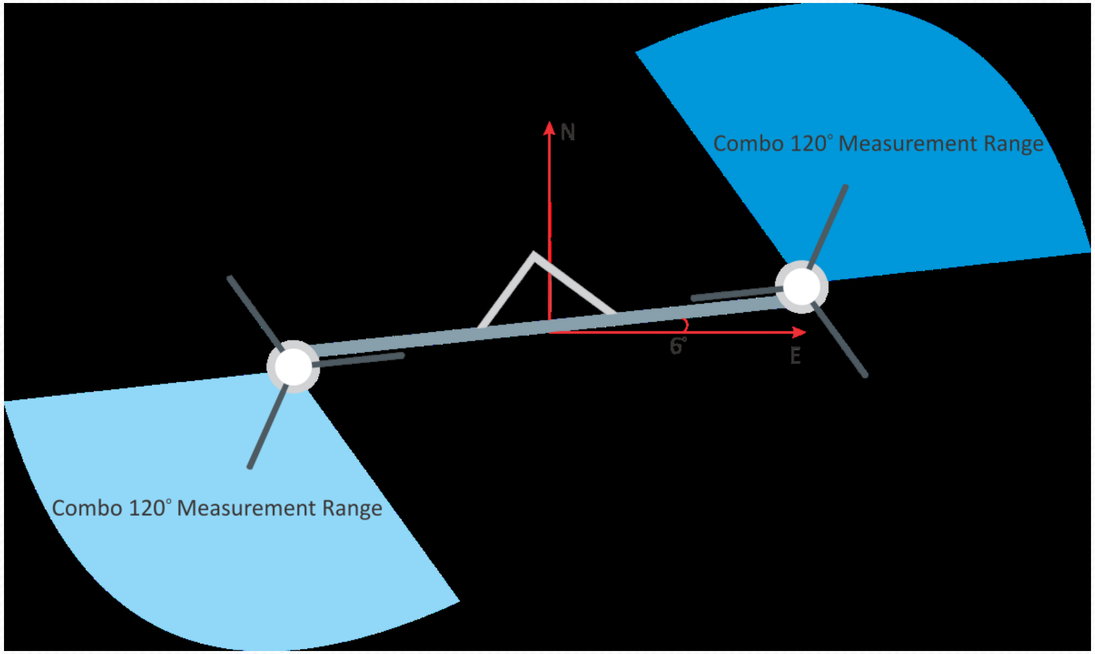

B

ES2 tower with combo probes positioned at 2 and 6 m.

A

B

Characteristic lengths during evening transition

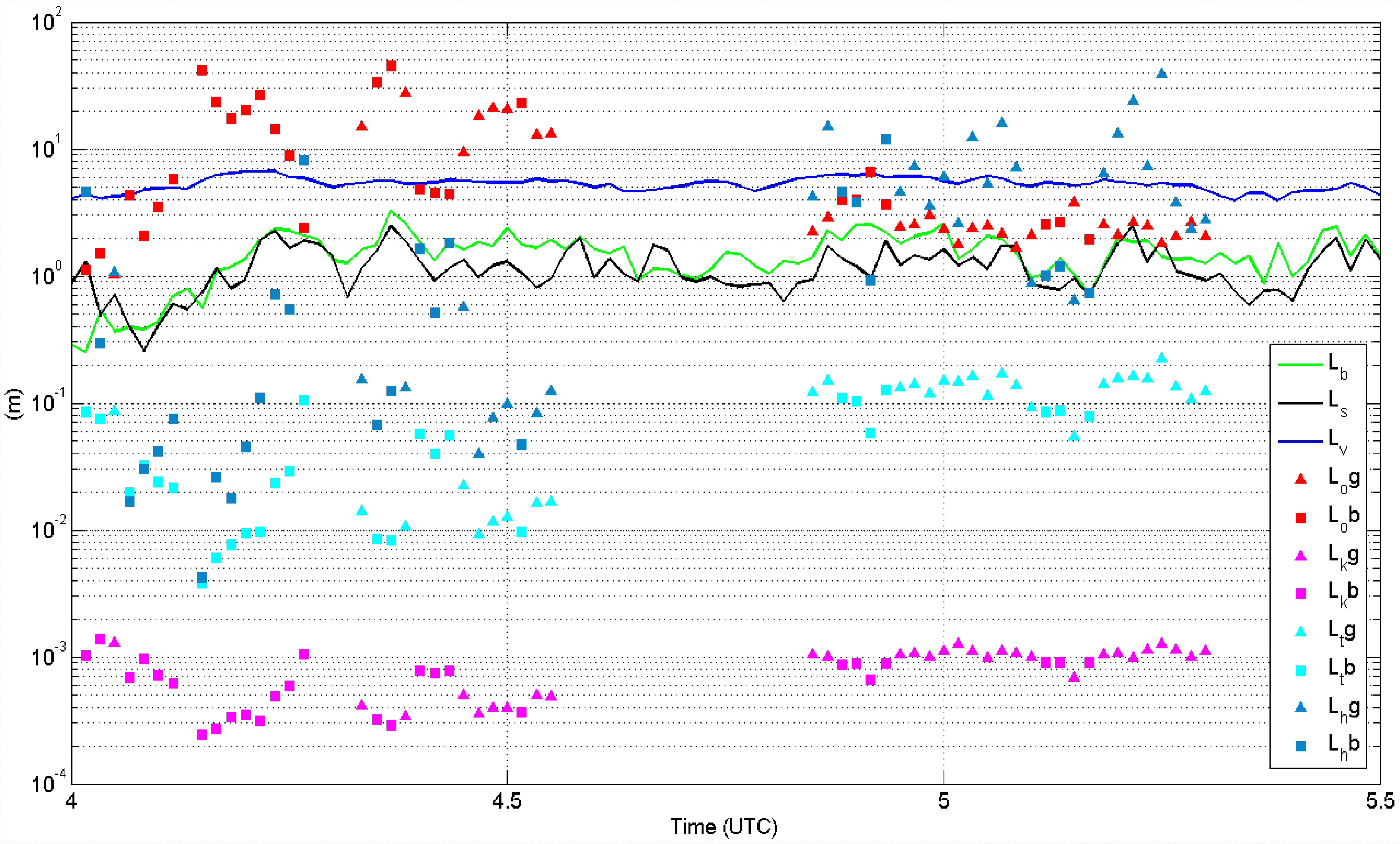

One-minute spectra and characteristic length scales

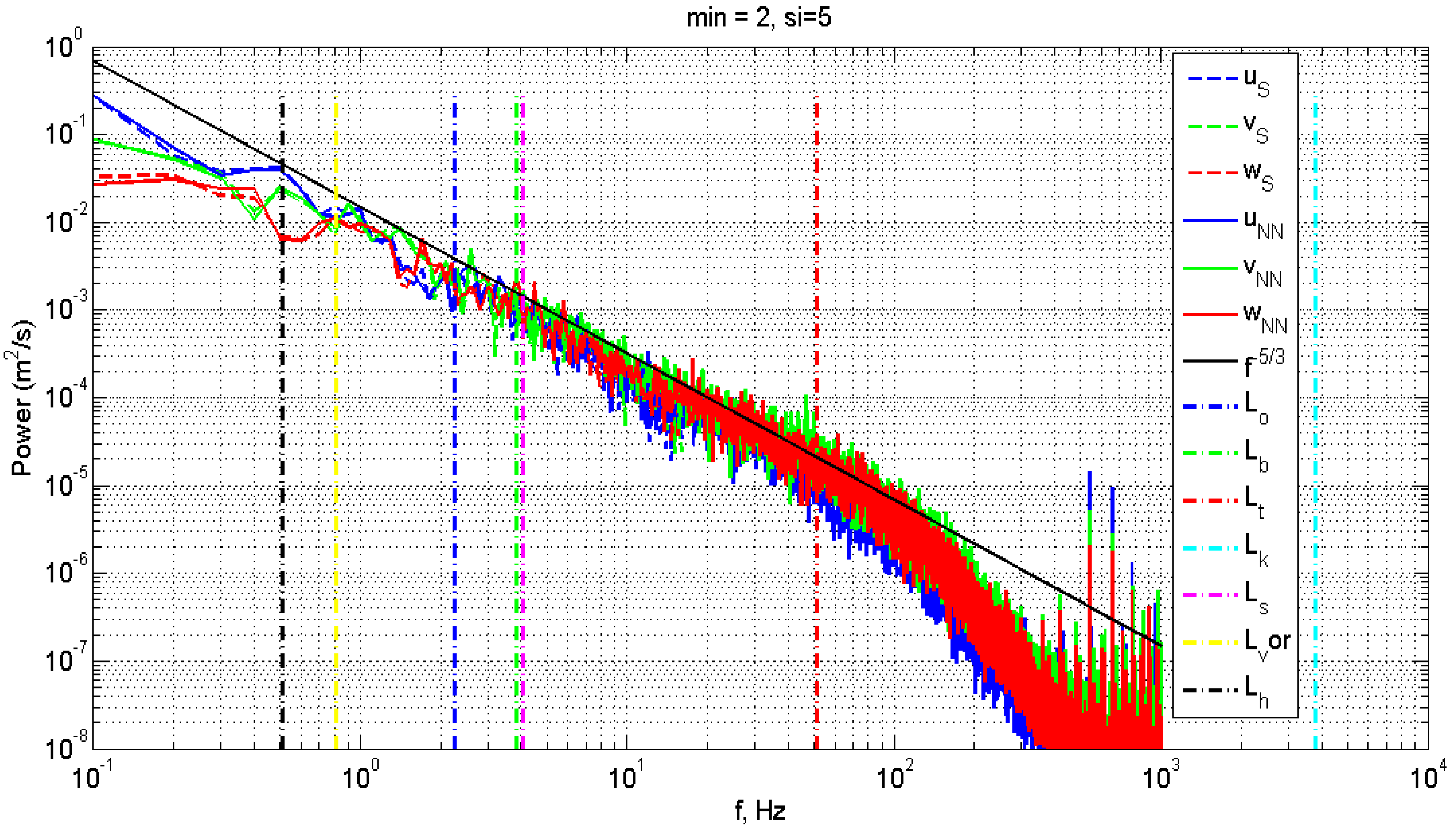

One-minute spectra and characteristic length scales

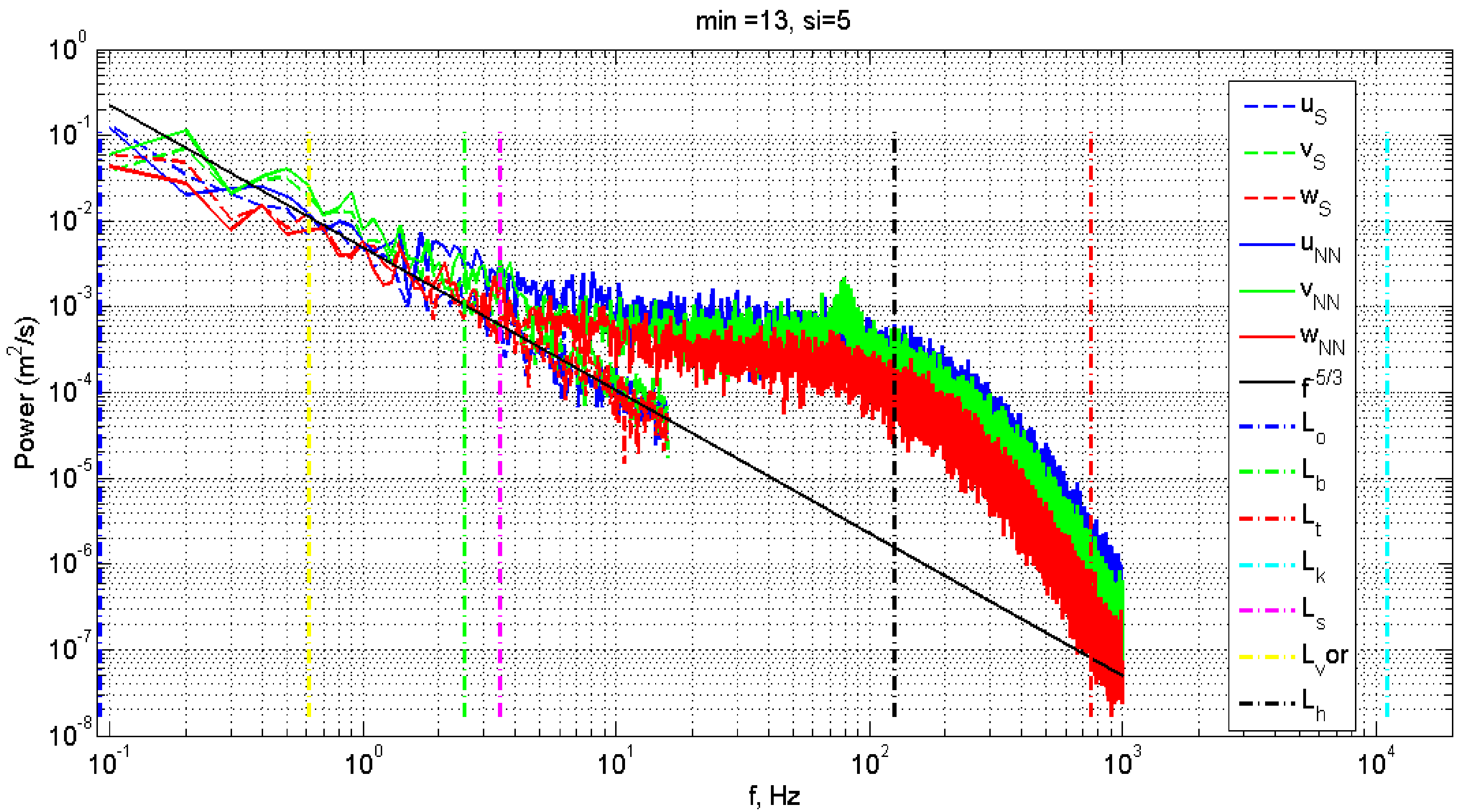

- **VIRTUAL PROBE ALGORITHM**

Virtual Probe

Determination of virtual probe parameters

- Calculation of the "effective " cooling velocity using calibration data-set previously measured (Kit et al., 2010)

$$U_{eff}^2 = U_n^2 + k^2 U_t^2$$

- Found best fit for King's law coefficients A, B and the power n

$$E^2 = A + B \cdot U_{eff}^n$$

Computation of simulated voltages

- Calculation of the "effective" cooling velocity using measured or synthetic full velocity datasets

$$U_{eff}^2 = U_n^2 + k^2 U_t^2 + h^2 U_b^2$$

- Computation of simulated voltages employing King's law with earlier determined coefficients A, B and n

Virtual Probe contd.

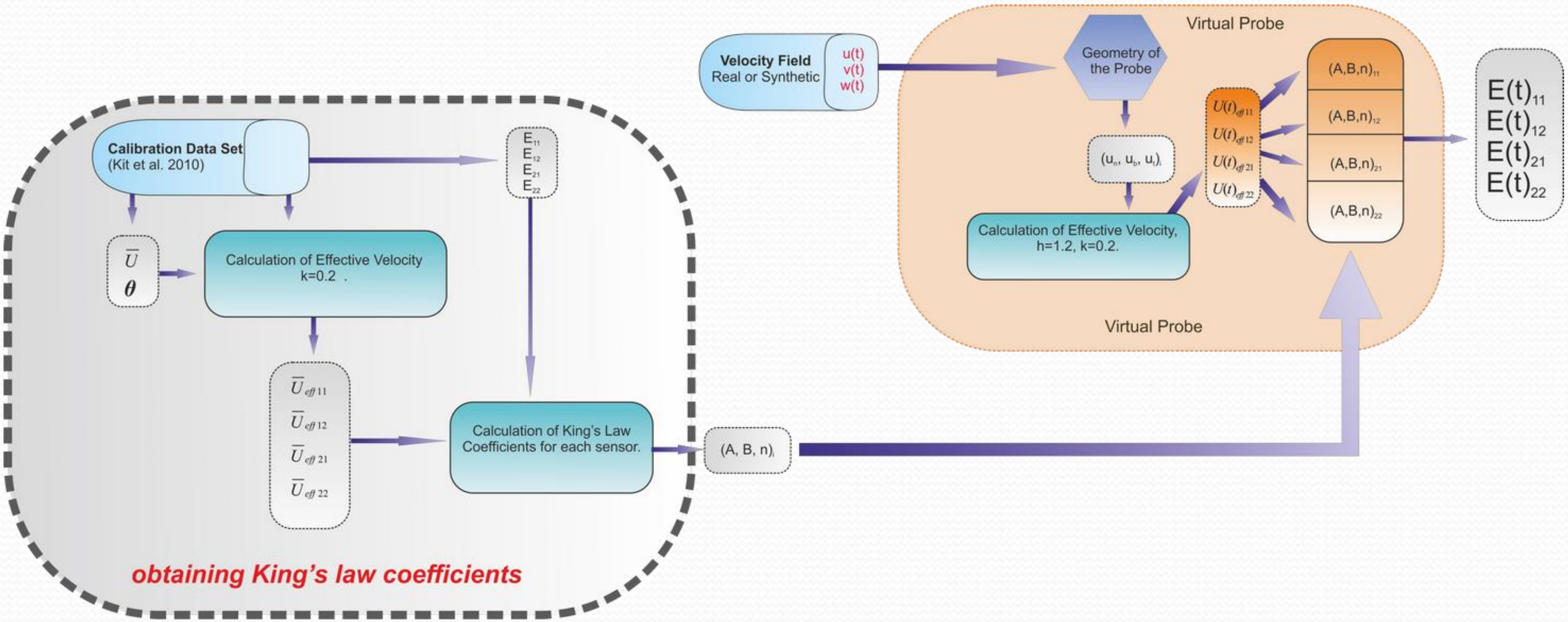

Conclusions

- Combo setup and Neural Network algorithm enable to obtain valuable information on the atmospheric flow especially during the transition events.
- Careful analysis is needed to select appropriate calibration datasets and time series for data processing
- The extrapolation of spectra based on Sonic data only can lead to a faulty conclusions as was indicated by velocity spectra obtained from combo measurements.
- There is indication that the use of four-sensor probes may be of advantage and can improve the signal-to-noise ratio due to redundant information.
- Further analysis of the spring data is in progress and hopefully will provide new perception

Conclusions

- NN model works with calibration datasets with unevenly distributed data points, PF works only with evenly.
- Field: Nocturnal works best and recommended.
- Very interesting spectra in our short preliminary campaign.
- Model of Angular Density Probability (ADP) is developed based on Gaussian distribution of velocity components.
- Angular Probability Distribution for calibration dataset is twice as narrow as for full signal. PF fails, NN comes through.
- Studying of non-linearity defined as RMS to mean velocity ratio
- Further development of the method: establishing of criteria for data quality.